Molkenthin, C., Scherbaum, F., Griewank, A., Leovey, H., Kucherenko, S., Cotton, F. (2017): Derivative-Based Global Sensitivity Analysis: Upper Bounding of Sensitivities in Seismic-Hazard Assessment Using Automatic Differentiation. - *Bulletin of the Seismological Society of America*, *107*, 2, pp. 984—1004.

DOI: http://doi.org/10.1785/0120160185

THE SEISMOLOGICAL SOCIETY OF AMERICA
400 Evelyn Ave., Suite 201
Albany, CA 94706-1375
(510) 525-5474; FAX (510) 525-7204
www.seismosoc.org

Bulletin of the Seismological Society of America, Vol. 107, No. 2, pp. 984–1004, April 2017, doi: 10.1785/0120160185

Derivative-Based Global Sensitivity Analysis: Upper Bounding of Sensitivities in Seismic-Hazard Assessment Using Automatic Differentiation

by Christian Molkenthin,[*] Frank Scherbaum,[*] Andreas Griewank,[†] Hernan Leovey,[‡] Sergei Kucherenko, and Fabrice Cotton[§]

Abstract Seismic-hazard assessment is of great importance within the field of engineering seismology. Nowadays, it is common practice to define future seismic demands using probabilistic seismic-hazard analysis (PSHA). Often it is neither obvious nor transparent how PSHA responds to changes in its inputs. In addition, PSHA relies on many uncertain inputs. Sensitivity analysis (SA) is concerned with the assessment and quantification of how changes in the model inputs affect the model response and how input uncertainties influence the distribution of the model response. Sensitivity studies are challenging primarily for computational reasons; hence, the development of efficient methods is of major importance. Powerful local (deterministic) methods widely used in other fields can make SA feasible, even for complex models with a large number of inputs; for example, automatic/algorithmic differentiation (AD)-based adjoint methods. Recently developed derivative-based global sensitivity measures can combine the advantages of such local SA methods with efficient sampling strategies facilitating quantitative global sensitivity analysis (GSA) for complex models.

In our study, we propose and implement exactly this combination. It allows an upper bounding of the sensitivities involved in PSHA globally and, therefore, an identification of the noninfluential and the most important uncertain inputs. To the best of our knowledge, it is the first time that derivative-based GSA measures are combined with AD in practice. In addition, we show that first-order uncertainty propagation using the delta method can give satisfactory approximations of global sensitivity measures and allow a rough characterization of the model output distribution in the case of PSHA. An illustrative example is shown for the suggested derivative-based GSA of a PSHA that uses stochastic ground-motion simulations.

Introduction

Seismic-hazard assessment is of great importance for various applications within the field of engineering seismology, earthquake-resistant design, and seismic risk assessment. The current practice for estimating the seismic hazard at a given site is the application of probabilistic seismic-hazard analysis (PSHA; Cornell, 1968; McGuire, 2004). Having a clear understanding of which parameters drive the hazard results under various circumstances is crucial, especially for the applications that build upon PSHA. Sensitivity analysis (SA) aims to assess and quantify how changes in the model inputs affect the model output. Therefore, SA is a useful tool as it can identify which inputs are noninfluential and which are critical and thus provide insight into the model characteristics.

There is a wide range of SA methods and potentially useful sensitivity measures for models (see, e.g., Sobol', 1990; Saltelli *et al.*, 2000, 2008; Oakley and O'Hagan, 2004; Sobol' and Kucherenko, 2009; Iooss and Lemaître, 2015; Razavi and Gupta, 2015; Borgonovo and Plischke, 2016). A challenge linked to SA is the required computational effort, which can be excessive or prohibitive for complex models, depending on the applied SA method (Iooss and Lemaître, 2015; Razavi and Gupta, 2015). SA methods are generally categorized into two groups, based either on local (deterministic) or global (often

[*]Also at German Research Center for Geosciences (GFZ), 14476 Potsdam, Germany; cmolke@gfz-potsdam.de, frank.scherbaum2@gfz-potsdam.de.

[†]Also at Department of Mathematics, Humboldt-University Berlin, Unter den Linden 6, 10099 Berlin, Germany; griewank@math.hu-berlin.de.

[‡]Now at Structured Energy Management Team, Axpo, Parkstrasse 23, CH-5401 Baden, Switzerland; hernaneugenio.leoevey@axpo.com.

[§]Also at Institute of Earth and Environmental Science, University of Potsdam, Karl-Liebknecht Street 24-25, 14476 Potsdam, Germany.

sampling based, statistical) concepts for carrying out sensitivity and uncertainty analysis (Cacuci and Ionescu-Bujor, 2004; Ionescu-Bujor and Cacuci, 2004).

Local SA methods aim to quantify the change of the model output due to small perturbations of the inputs at a reference point (often called base case) in the input space. Local sensitivity estimates are only valid in the vicinity of the reference point considering (small) input perturbations, for which nonlinearity in the input–output relation can be neglected. In the case of a linear or nearly linear model, first-order uncertainty analysis based on partial derivatives (local sensitivities) can be sufficient for quantifying the global sensitivity of the complete input domain in a very simple way. An advantage of local SA methods is that they can be very efficient in providing sensitivities even for complex models; for example, using the adjoint method based on automatic/algorithmic differentiation (AD; Griewank and Walther, 2008). A computer source code representation of the model is sufficient and AD can be applied directly. Many computer models can have kinks or even jumps so that local sensitivities in the sense of derivatives are not defined. The approximation of such functions by piecewise linear functions has recently been proposed by Griewank (2013).

Global sensitivity analysis (GSA) methods have the aim of quantifying the influence that the uncertainty of a particular input or group of inputs (over its entire range) has on the model response. It is typically based on the analysis (usually statistical summaries) of many model evaluations (or their partial derivatives) on randomized input samples taken over the complete input domain. A large spectrum of qualitative and quantitative GSA methods exist (summarized in Oakley and O'Hagan, 2004; Saltelli *et al.*, 2008; Sobol' and Kucherenko, 2009; and Borgonovo and Plischke, 2016); for example, Morris method, sequential bifurcation, analysis of the variance, regression-based methods, methods using surrogate models, methods analyzing changes in the density and cumulative density function, entropy-based methods, derivative-based methods, and Bayesian methods.

The most popular quantitative GSA method is the variance-based approach, often referred to as the Sobol' method, a decomposition of the total variance of the output into terms of contributions of partial variances of the individual input variables or groups of input variables (Sobol', 2001; Saltelli, 2002). Variance-based GSA has been applied successfully in many SA studies of models and is often taken as a standard benchmark test when performing comparison of different GSA methods (e.g., Borgonovo, 2006; De Rocquigny *et al.*, 2008; Saltelli *et al.*, 2008; Massmann and Holzmann, 2012; Plischke *et al.*, 2013; Rakovec *et al.*, 2014). The major challenge for quantitative sampling-based GSA methods, including Sobol' method, is that they may require a large number of model evaluations to estimate the GSA measures or indicators; consequently, those methods are normally restricted to low-dimensional models ($<$ 10–20 inputs) and/or to models with short run times (Iooss and Lemaître, 2015).

Given the number of above-mentioned SA approaches, the choice of which particular SA method should be applied strongly depends on the nature of the question to be addressed as well as on practical computational aspects. In this study, we mainly focus on GSA of the seismic hazard produced by PSHA. Knowledge of local sensitivities (partial derivatives) at several reference points (sample points of the input domain) can significantly reduce the computational effort for obtaining GSA measures (Sobol' and Kucherenko, 2009; Rakovec *et al.*, 2014). This makes the application of sampling-based GSA also possible for models with a large number of inputs. It was recently shown that globally aggregated partial derivatives (local sensitivities) yield an upper bounding of global parameter sensitivities, which in turn allows the identification of noninfluential uncertain inputs (Sobol' and Kucherenko, 2009; Lamboni *et al.*, 2013). Subsequently, these inputs could be fixed at their nominal value (e.g., expectation), reducing the model complexity. Furthermore, the obtained global upper bounds can be used to rank influential inputs as done in variance-based GSA measures (reference method) in the case of linear, nearly linear, or product functions (Rakovec *et al.*, 2014; Kucherenko and Iooss, 2016). However, derivative-based GSA requires partial derivatives at several sample points, whose evaluation can be challenging and computationally very demanding or even infeasible for complex models.

In this study, we propose to combine derivative-based GSA with AD to overcome this problem. AD is a powerful approach that allows the evaluation of derivatives of complex models accurately and most efficiently (Griewank and Walther, 2008). Hence, the suggested GSA approach is computationally feasible for models with a greater number of inputs. It enables an upper bounding of the sensitivities globally, and, therefore, an identification of noninfluential and most dominant uncertain inputs involved in PSHA. We present an illustrative example of the proposed derivative-based SA approach relying on AD in a sensitivity study of a PSHA for an area source. Within the PSHA, we employ the stochastic simulation technique (e.g., Boore, 2003) for the prediction of ground motion. (1) Results of local SA are presented to show how small changes (e.g., $\leq$5%) in the inputs influence the model response. (2) Two sets of results of derivative-based GSA are presented to assess how input uncertainties affect the distribution of the model response. (a) We show global upper bounds on the input sensitivities. (b) Moreover, we show that GSA results obtained via the classical first-order uncertainty propagation (delta method) can give satisfactory approximations of global sensitivity measures in the case of PSHA. Thus, we can identify the inputs whose uncertainty plays a significant role. We compare against results obtained from a simple graphical GSA method (scatter plots) and from a widely used quantitative reference method (variance-based GSA) to verify consistency of the results.

Sensitivity Analysis Methods and Automatic Differentiation

Local Sensitivity Analysis and Automatic Differentiation

Local SA assesses how small changes in the inputs of a model influence the model response. Consider a deterministic model given as

$$y = f(\mathbf{x}), \qquad \mathbf{x} \in \mathbb{R}^k, \tag{1}$$

with k inputs $\mathbf{x} = [x_1, x_2, \ldots, x_k]$ and for simplicity with a scalar-valued model response y. (In this study, it is the annual rate of exceedance of a particular ground-motion level or the ground-motion level given an annual rate of exceedance.) Local sensitivities are mathematically defined as the partial derivatives of the model output with respect to its inputs at reference point $\mathbf{x}_0$ as follows:

$$d_i = \left.\frac{\partial f(\mathbf{x})}{\partial x_i}\right|_{\mathbf{x}_0}, \tag{2}$$

in which d_i is the local absolute sensitivity of the ith input. However, partial derivatives (d_i) are often not comparable because the different units or scales of the inputs make a ranking of the inputs difficult. To avoid related problems, one usually employs relative sensitivities (also called logarithmic sensitivities or elasticities) for this issue which are defined as follows:

$$d_i^{\mathrm{rel}} = \left.\frac{\partial f(\mathbf{x})}{\partial x_i}\right|_{\mathbf{x}_0} \frac{x_{0,i}}{y_0}, \tag{3}$$

in which $x_{0,i}$ is the ith component of $\mathbf{x}_0$ and $y_0 = f(\mathbf{x}_0)$. Therefore, relative sensitivities relate proportional changes. Usually, the same proportional perturbation (same relative error) for all inputs is assumed and one estimates the corresponding proportional change in the model response. For d_i^{rel} to be defined, the model output y_0 must be nonzero. The magnitude of the absolute value of the relative sensitivities $|d_i^{\mathrm{rel}}|$ is taken as indicator for the importance of the different inputs.

In general, the local behavior of the model is approximated by a first-order Taylor expansion at $\mathbf{x}_0$ assuming that higher order terms can be neglected. Such local first-order estimates are generally not valid for parameter ranges far away from the reference point unless the model is linear or nearly linear. However, local sensitivities give valuable information for several applications in optimization and simulation, for example, parameter identification of nonlinear inverse problems, and they are the basis for differential SA. In the case of uncertain inputs, as we explain in detail in the Global Sensitivity Analysis section, some functionals of the partial derivatives are used to form an upper bound on parameter sensitivities. Alternatively, if the model is nearly linear, the partial derivatives (always at a base case $\mathbf{x}_0$) can be used for first-order uncertainty propagation (delta method).

The most challenging part in this context is the computation of the partial derivatives, as their evaluation can be problematic in terms of accuracy and computational effort. Partial derivatives can be obtained manually, which is usually not possible for complex models, or numerically as divided differences. Divided difference techniques suffer from accuracy problems and become computationally expensive for complex models with many inputs because the computational effort increases linearly with the number of inputs. However, there exists a third method which can procure partial derivatives efficiently even for complex models, namely AD. AD has recently gained much attention in different scientific domains such as statistical parameter estimations (Fournier *et al.*, 2012; Skaug and Yu, 2014), applications in machine learning (Baydin *et al.*, 2015), and SA and parameter identification in hydrology (Castaings *et al.*, 2009). The first applications using AD in seismology are due to Sambridge *et al.* (2007) and Molkenthin *et al.* (2014).

AD is a chain-rule-based method that allows the differentiation of computer source code (i.e., the numerical representation of the model) by compiler-like AD tools that automatically produce new augmented source code that additionally calculates the required derivatives. In this work, we employ a source code transforming AD tool. The resulting program delivers the model output and, simultaneously, all required partial derivatives of the model output with respect to its inputs. AD is directly applied to the numerical implementation of the model. The basic idea is that any numerical code of a model can be seen as a composition of a finite sequence of elementary calculations or instructions computing a chain of intermediate values before the final output is obtained. The chain rule of differential calculus can be applied to this composition in an automatic manner to obtain a differentiated version of the original numerical computer code of the model. One distinguishes between two modes of AD: one is the forward mode (forward application of the chain rule) and the other is the reverse mode (backward application of the chain rule). The resulting differentiated model of the forward mode is called the tangent-linear model (TLM), whereas the one of the reverse mode is called the adjoint model (ADM). The computational costs for the calculation of the partial derivatives by TLM increase linearly with the number of inputs $O(k)$. In contrast, using ADM in the case of a scalar-valued output, one can compute the complete gradient of the model response independently of the number of inputs with a minimal overhead $O(c)$, which is a small factor (usually $c < 6$) times the original forward computation of the function itself (Griewank and Walther, 2008). There are currently several source code transforming AD tools available for different programming languages. A link for a comprehensive overview of AD tools and AD methodology as well as AD applications is given in Data and Resources.

AD was recently employed as a tool for carrying out sensitivity analyses in the context of seismic hazard and ground-motion modeling in Molkenthin *et al.* (2014, 2015). Here, we build upon these works and use the differentiable source codes developed therein. These source codes are written in FORTRAN, and their differentiated versions were obtained using the Tapenade AD tool (Hascoet and Pascual, 2013).

Global Sensitivity Analysis

Consider a deterministic computer model $f(\boldsymbol{X})$ with k uncertain inputs $\boldsymbol{X} = [X_1, X_2, \ldots, X_k]$ yielding a distribution Y of a scalar model output:

$$Y = f(\boldsymbol{X}) = f(X_1, X_2, \ldots, X_k), \qquad \boldsymbol{X} \in \mathbb{R}^k. \tag{4}$$

The uncertain inputs $\boldsymbol{X}$ are treated as random variables, characterized by their corresponding density functions $X_i \sim \mu_i(x)$ for each input i. The term deterministic means that the same set of input values $\boldsymbol{x} = [x_1, x_2, \ldots, x_k]$ as a realization of the input random variables in $\boldsymbol{X}$ will produce exactly the same model output $y = f(\boldsymbol{x})$. Accordingly, the distribution Y is induced by the given densities of $\boldsymbol{X}$. The considered scalar model output y in this study is, for example, the level of expected shaking in terms of a response spectral ordinate at a fixed oscillator frequency given a return period (level of safety).

GSA provides valuable information on how uncertainties in the inputs influence the model output by varying all inputs jointly. Quantitative GSA intends to apportion the model output uncertainty to the different sources of the input uncertainties in order to identify important and noninfluential inputs (Saltelli *et al.*, 2000). Measures of global sensitivities rely on statistics gathered from evaluating the model (or its derivatives) on inputs sampled from their corresponding distribution. There are different global sensitivity measures and one has to keep in mind that different GSA methods may result in a different importance ranking of the inputs, as demonstrated, for example, in Pappenberger *et al.* (2008). The most important step in GSA is the assignment of distributions $\mu_i(x)$ to the uncertain inputs X_i. Therefore, the characterization of the input uncertainties has to be done with utmost caution, and is typically based on data and expert knowledge.

To perform sampling-based GSA, we require an efficient sampling method. There are several possible sampling procedures; for example, classical Monte Carlo (MC) sampling and Latin hypercube sampling. Here, we suggest using quasi-MC sampling because it often performs better than classical MC methods (Kucherenko *et al.*, 2011, 2015). The efficiency of MC methods is determined by the properties of random numbers. It is known that random number sampling is prone to clustering: for any sampling there are always empty areas as well as regions in which random points are wasted due to clustering. As new points are added randomly, they do not necessarily fill the gaps between already sampled points. A higher rate of convergence can be obtained by using deterministic uniformly distributed sequences, also known as low-discrepancy sequences (LDS), instead of pseudorandom numbers. Methods based on the usage of such sequences are known as quasi-MC methods (Niederreiter, 1992). LDS are specifically designed to place sample points as uniformly as possible. Unlike random numbers, successive LDS points know about the position of previously sampled points and fill the gaps between them. LDS are also known as quasi-random numbers. There are a few well-known and commonly employed LDS. Different principles were used for their construction by Holton, Faure, Sobol', Niederreiter, and others. Many practical studies have proven that the Sobol' LDS is in many aspects superior to other LDS (Bratley *et al.*, 1992; Paskov and Traub, 1995; Sobol', 1998; Kucherenko *et al.*, 2011, 2015). For this reason it was used in this work.

Table 1
Measures Used for Global Sensitivity Analysis (GSA)

Measure	Sampling	Computational Costs
Main effect S_i, total effect S_{T_i}	Yes	$N_S(k+2)$
Upper bound for the total effect U_i	Yes	cN_{U_i}
Delta method GSA measure $\hat{S}_i^L$	No	c

The computational costs are measured in terms of required model evaluations.

N_{U_i} (N_S), the number of required sample points to estimate GSA measures U_i (S_i, S_{T_i}); k, number of inputs; c, a small constant (usually $c \leq 6$).

A challenge for quantitative GSA methods (including Sobol' method) is that they require a large number of model evaluations to estimate the GSA measures or indicators. Therefore, applying those methods can be computationally very demanding and prohibitive for complex models with many inputs or long run times. To overcome these limitations, we will focus on derivative-based GSA.

In the following, we briefly give an overview of (1) the classical variance-based GSA method (also called Sobol' method), which is taken as a reference method to evaluate our results, before presenting (2) the suggested derivative-based GSA method, which is a simple and computationally much cheaper alternative to (1). Subsequently, the delta method (first-order uncertainty propagation) and related first-order GSA estimates are briefly described. Employed GSA measures, which are explained in the following subsections, are summarized in Table 1.

Variance-Based GSA. The most often used GSA method is a variance-based GSA that aims to decompose the total variance of the model output Var[Y] into contributions of the individual inputs (or sets of inputs) and contributions of their interactions. The importance of an input is assessed in terms of its contribution to the model output variance. At the same time, it refers to the possible reduction of the model output variance if the input would be known with certainty. All the following explanations are valid for individual inputs as well as for sets (groups) of inputs.

A classical approach in variance-based GSA is based on analysis of variance (ANOVA) decomposition introduced by Sobol' (1990). It can be shown that the same expressions for global sensitivity indexes can be obtained using the basic expression for the decomposition of Var[Y] with respect to an input X_i using the law of total variance:

$$\mathrm{Var}[Y] = \mathrm{Var}_{X_i}[\mathrm{E}_{\boldsymbol{X}_{\sim i}}[Y|X_i]] + \mathrm{E}_{X_i}[\mathrm{Var}_{\boldsymbol{X}_{\sim i}}[Y|X_i]] \tag{5}$$

(McKay, 1995), in which the variance of Y is decomposed into two terms on the right side: the explained output

variance due to a dependency upon input X_i (first term) and an unexplained remaining (residual) fraction of variance in Y due to other inputs or interactions between other inputs and X_i (latter term). $\mathrm{Var}_{X_i}[\mathrm{E}_{\boldsymbol{X}_{\sim i}}[Y|X_i]]$ is the variance of the conditional expectation and $\mathrm{E}_{X_i}[\mathrm{Var}_{\boldsymbol{X}_{\sim i}}[Y|X_i]]$ is the expectation of the conditional variance (residual part), both conditioned on x_i. The subscripts X_i and $\boldsymbol{X}_{\sim i}$ denote where the variance or the expectation is taken over, and $\boldsymbol{X}_{\sim i}$ means all inputs other than X_i. Given equation (5), a possible measure for the reduction of $\mathrm{Var}[Y]$, if input X_i could be fixed, is

$$V_i = \mathrm{Var}_{X_i}[\mathrm{E}_{\boldsymbol{X}_{\sim i}}[Y|X_i]], \tag{6}$$

in which V_i is called the partial variance of the input X_i. V_i is used as a measure of the importance or influence of input X_i on the variance of Y: the larger the V_i the larger the global sensitivity of X_i. To obtain a scale invariant global sensitivity measure S_i between 0 and 1, V_i is normalized by $\mathrm{Var}[Y]$:

$$S_i = \frac{V_i}{\mathrm{Var}[Y]}, \tag{7}$$

in which S_i is the first-order global sensitivity index (also called first-order Sobol' index) measuring the main effect of input X_i on the model output Y. The relative importance of each input is given by its main effect (first-order Sobol' index) S_i, representing the greatest potential (largest S_i) for reducing the variance of the model response $\mathrm{Var}[Y]$. S_i does not consider input interactions. If the sum of all S_i: $\left(\sum_{i=1}^{k} S_i\right)$ is close to one, it indicates that there are only minor interaction effects and the model is additive as defined within the ANOVA framework.

The second principle measure in variance-based GSA, proposed by Homma and Saltelli (1996), is related to the remaining uncertainty in Y; that is, the uncertainty that is left unexplained after we fixed all inputs except X_i. This residual variance V_{Ti} due to X_i and all its interactions using the total law of variance is

$$V_{Ti} = \mathrm{Var}[Y] - \mathrm{Var}_{\boldsymbol{X}_{\sim i}}[\mathrm{E}_{X_i}[Y|\boldsymbol{X}_{\sim i}]]. \tag{8}$$

Dividing V_{Ti} by $\mathrm{Var}[Y]$ gives the scale invariant global sensitivity measure S_{Ti} called total effect of input X_i:

$$S_{Ti} = \frac{V_{Ti}}{\mathrm{Var}[Y]}. \tag{9}$$

Note, due to the fact that interaction terms are counted several times, the sum of all S_{Ti} $\left(\sum_{i=1}^{k} S_{Ti} \geq 1\right)$ can become larger than 1. The total effect S_{Ti} is a measure for the portion of the model output variance, which can be attributed to all effects in which input X_i is involved. Thus, the total sensitivity index S_{Ti} can help us identify noninfluential inputs: a low value of S_{Ti} (e.g., $S_{Ti} \ll 1/k$ with k number of inputs) indicates that the input X_i is noninfluential and can be fixed (e.g., $x_i = \mathrm{E}[X_i]$).

In general, assuming k independent inputs X_i, the total variance $\mathrm{Var}[Y]$ of the model response can be decomposed into $2^n - 1$ components:

$$\mathrm{Var}[Y] = \sum_{i=1}^{d} V_i + \sum_{i=j}^{d} V_{ij} + \cdots + V_{12\ldots d} \tag{10}$$

(Sobol', 2001), in which V_i represents the first-order terms, V_{ij} are the second-order terms, and so on. Subsequently, global sensitivity measures of different orders can be obtained by computing the ratio between these partial variances and the total variance of the model output $S_{i_1,\ldots,i_k} = \frac{V_{i_1,\ldots,i_k}}{\mathrm{Var}[Y]}$. Such higher order global sensitivity indexes account for interactions between one or more inputs. In practice, computing the two sets of k global sensitivity indexes (S_i and S_{Ti} for each input $i = 1, 2, \ldots, k$) often provides sufficient information to obtain the global sensitivities of the model output with respect to the individual inputs (Saltelli *et al.*, 2010). In the numerical example, S_i and S_{Ti} are used as reference measures for evaluating the proposed approach.

The computation of the variance-based GSA indexes S_i and S_{Ti} involves evaluating several multidimensional integrals, which are approximated using MC methods. There exist several ways for approximating these integrals based on classical MC sampling or quasi-MC sampling (e.g., Homma and Saltelli, 1996; Saltelli, 2002; Saltelli *et al.*, 2010; Kucherenko *et al.*, 2011). Correspondingly, first-order Sobol' indexes S_i together with S_{Ti} can be calculated with a cost of $N_S(k+2)$ model evaluations, in which N_S is the number of required samples, and k is the number of inputs. As explained earlier, in this study we employ quasi-MC sampling using LDS (i.e., Sobol' sequence in our case, Sobol' *et al.*, 2011) in connection with formulas for S_i and S_{Ti} in Sobol' (2001) and Sobol' *et al.* (2007, 2011). S_i and S_{Ti} are estimated as follows: an initial sampling matrix (quasi-MC samples) of size $(N_S, 2k)$ is generated from a Sobol' sequence containing values ranging from zero to one. This initial matrix is divided into two sample matrices $\mathbf{A}$ and $\mathbf{B}$ in such a way that the left half (column one to k) is matrix $\mathbf{A}$ and the right half (column $(k+1)$ to $2k$) is matrix $\mathbf{B}$. Subsequently, inverse sampling theorem is applied to obtain input samples accordingly to the assigned densities (μ_i) with values in their actual range. Then, based on the two sampling matrices $\mathbf{A}$ and $\mathbf{B}$, each of size (N_S, k), one generates additional k matrices $\mathbf{A}_{\mathbf{B}}^{(i)}$ of the same size in such a way that matrix $\mathbf{A}_{\mathbf{B}}^{(i)}$ is identical to matrix $\mathbf{A}$, except that its ith column is replaced by the ith column of matrix $\mathbf{B}$. Subsequently, the model f is evaluated for each row of the $k+2$ matrices, yielding the vectors $f(\mathbf{A}) \in R^{N_S}, f(\mathbf{B}) \in R^{N_S}, f(\mathbf{A}_{\mathbf{B}}^{(1)}) \in R^{N_S}, , \ldots, f(\mathbf{A}_{\mathbf{B}}^{(k)}) \in R^{N_S}$. Finally, the index S_i of the ith input is empirically estimated (denoted by $\hat{S}_i$) as follows:

$$\hat{S}_i = \frac{\mathrm{Var}_{X_i}[\mathrm{E}_{\boldsymbol{X}_{\sim i}}[Y|X_i]]}{\mathrm{Var}[Y]} = \frac{\frac{1}{N_S}\sum_{j=1}^{N_S} f(\mathbf{B})_j (f(\mathbf{A}_B^{(i)})_j - f(\mathbf{A})_j)}{\mathrm{Var}[Y]}, \tag{11}$$

and S_{Ti} as

$$\hat{S}_{Ti} = 1 - \frac{\mathrm{Var}_{X_{\sim i}}[\mathrm{E}_{X_i}[Y|\boldsymbol{X}_{\sim i}]]}{\mathrm{Var}[Y]} = \frac{\frac{1}{2N_S}\sum_{j=1}^{N_S}(f(\mathbf{A})_j - f(\mathbf{A}_B^{(i)})_j)^2}{\mathrm{Var}[Y]}, \tag{12}$$

in which $(\mathbf{A})_j$, $(\mathbf{B})_j$, and $(\mathbf{A}_B^{(i)})_j$ denote the jth row of matrices $\mathbf{A}$, $\mathbf{B}$, and $\mathbf{A}_B^{(i)}$, respectively, and where all products among vectors are to be understood as Euclidean scalar vector products.

Derivative-Based GSA. In this study, we suggest combining an efficient local sensitivity method (adjoint AD methods) with a powerful global sampling approach (quasi-MC sampling) to obtain globally aggregated local sensitivity information that makes derivative-based GSA possible for complex models. Small first-order derivatives of a function imply small total Sobol' sensitivity indexes S_{Ti}. This fact can be used for a global upper bounding of sensitivities. Simply put, these upper bounds U_i are obtained by averaging the squared partial derivatives (local sensitivities) of the model output over the input domain at different sample points. These expectation values $\mathrm{E}[(\frac{\partial f(\mathbf{x})}{\partial x_i})^2]$ (one for each input) are multiplied by a specific constant C_{μ_i}, which depends on the type of the density function μ_i (Sobol' and Kucherenko, 2009; Lamboni *et al.*, 2013). This gives an upper bound U_i on S_{Ti}:

$$S_{Ti} \le U_i, \tag{13}$$

in which U_i for each input i reads as follows:

$$U_i = C_{\mu_i}\frac{\int_{\mathbb{R}^k}\left(\frac{\partial f(\mathbf{x})}{\partial x_i}\right)^2\mu(\mathbf{x})d\mathbf{x}}{\mathrm{Var}[f(\boldsymbol{X})]} = C_{\mu_i}\frac{\mathrm{E}\left[\left(\frac{\partial f(\mathbf{x})}{\partial x_i}\right)^2\right]}{\mathrm{Var}[Y]}. \tag{14}$$

We assume that the probability measure P has a density μ of the form $\mu(\mathbf{x}) = \mathbf{\Pi}_{i=1}^k \mu_i(x_i)$ ($\mathbf{x} \in \mathbb{R}^k$), in which μ_i is a continuous (marginal) density on $\mathbb{R}$. The expectation E[.] of the squared partial derivatives of the ith input in equation (14) is usually denoted as ν_i referred by Sobol' and Kucherenko (2009) as the derivative-based global sensitivity measure (DGSM), and can be approximated as a finite sum over $j = 1, \ldots, N$ quasi-MC samples $\mathbf{x}^j$ (drawn from $\mu(\mathbf{x})$ using inverse transform sampling):

$$\hat{\nu}_i = \frac{1}{N}\sum_{j=1}^{N}\left(\frac{\partial f(\mathbf{x}^j)}{\partial x_i}\right)^2, \tag{15}$$

in which $\hat{\nu}_i$ is the empirically estimated value of ν_i.

Constants C_{μ_i} required for the global upper bounding of sensitivities have been derived analytically by Sobol' and Kucherenko (2009) and Lamboni *et al.* (2013) for the case of the uniform, normal, and some other log-concave distributions, see Table 2. Roustant *et al.* (2014) include the results to cases of truncated log-concave distributions on $[a, b]$.

For the often-used lognormal distribution, which is not log-concave, no constant C_{μ_i} can be stated. For lognormally distributed inputs, we suggest the following procedure for upper bounding the sensitivities. Instead of estimating

Table 2
Constants C_μ for Some Density Functions

Distribution	C_μ
Uniform $\mathcal{U}([a, b])$*	$(b-a)^2/\pi^2$
Normal $\mathcal{N}(\mu, \sigma^2)$*	σ^2
Exponential $\mathcal{E}(\lambda)$, $\lambda > 0$†	$4/\lambda^2$
Gumbel $\mathcal{G}(\mu, \beta)$, scale $\beta > 0$†	$(2\beta/\log 2)^2$
Weibull $\mathcal{W}(k, \lambda)$, shape $k \ge 1$, scale $\lambda > 0$†	$\{[2\lambda(\log 2)^{(1-k)/k}]/k\}^2$

*After Sobol' and Kucherenko (2009).
†After Lamboni *et al.* (2013).

$$\nu_i = \int_0^{+\infty}\left(\frac{\partial f(\mathbf{x})}{\partial x_i}\right)^2\mu(\mathbf{x})d\mathbf{x}, \tag{16}$$

for the ith input, we suggest in its place the quantity

$$\nu_i^* = \int_0^{+\infty}\left(\frac{\partial f(\mathbf{x})}{\partial x_i}\right)^2 x_i^2\mu(\mathbf{x})d\mathbf{x}, \tag{17}$$

which is obtained by considering a change of variables to the normal case and then applying the corresponding upper bounds as $U_i = \sigma_i^2\frac{\nu_i^*}{\mathrm{Var}[Y]}$, in which σ_i is the scale parameter of the lognormal distribution μ_i, assuming ν_i^* is finite. For the case of truncated lognormal densities, the same technique of change of variables can be applied to obtain the corresponding upper bounds.

Once the upper bounds U_i on the global sensitivities for all inputs have been obtained, the following criterion is suggested to decide whether an input is noninfluential:

$$U_i << \frac{1}{k}, \tag{18}$$

in which k is the number of inputs. If all k inputs were equally influential, each input would explain the same fraction of the total variance. Hence, uncertain inputs with bounds significantly lower than $1/k$ are identified as nonimportant and can be fixed.

To evaluate the required derivative values at the sample points, we suggest applying reverse-mode AD. The computational cost for computing all k upper bounds of the sensitivities U_i require essentially cN_{U_i} model evaluations, in which N_{U_i} is the number of sample points and c is a small constant (usually $c < 6$). We emphasize that these costs in terms of model evaluations are effectively independent of the number of inputs, ignoring the cost of quadrature summations to calculate expectations and variances. In addition, the number of required sample points N_{U_i} to achieve numerical convergence may be smaller in practice for DGSMs than the number of samples N_S for variance-based sensitivity measures.

Delta Method. In the case of a linear or a nearly linear model $f(\mathbf{x})$, the established delta method (first-order uncertainty propagation) can be used to propagate input uncertainty. GSA can also benefit from the delta method. The idea is to approximate the first two moments (expectation

and variance) of the uncertain model output based on the first two moments of the inputs using the partial derivatives of the model output with respect to its inputs. The underlying assumption is that the properties of a random variable can be sufficiently described by its first and second moment, and that higher moments (e.g., the third moment, also called skewness) are relatively small. In this work, the required partial derivatives are obtained via AD.

More specifically, a first-order Taylor expansion of $f(\mathbf{x})$ with k inputs evaluated at a reference point $\mathbf{x}_0$ is used to approximate the following model:

$$f(\mathbf{x}) = f(\mathbf{x}_0) + \nabla_x f(\mathbf{x})|_{\mathbf{x}_0}(\mathbf{x} - \mathbf{x}_0), \tag{19}$$

in which $\mathbf{x}_0 = \mathrm{E}[\boldsymbol{X}]$ is the expectation of $\boldsymbol{X}$ and $\nabla_x f(\mathbf{x})$ stands for the gradient of $f(\mathbf{x})$ with respect to the inputs (i.e., local sensitivities of the model output) $\mathbf{x}$ evaluated at $\mathbf{x}_0$. It is assumed that higher order terms in the Taylor expansion are negligible.

Thus, the approximated expectation of the model response is

$$\mathrm{E}[Y] \approx f(\mathbf{x}_0), \tag{20}$$

and the approximated variance of the model response is

$$\mathrm{Var}[Y] \approx (\nabla_x f(\mathbf{x})|_{\mathbf{x}_0})^T \Sigma_{XX} (\nabla_x f(\mathbf{x})|_{\mathbf{x}_0}), \tag{21}$$

in which Σ_{XX} is the covariance matrix of $\boldsymbol{X}$. Assuming independent inputs, the approximation given in equation (21) reduces to

$$\mathrm{Var}[Y] \approx \mathrm{Var}_L[Y] = \sum_{i=1}^{k} \left[\frac{\partial f(\boldsymbol{x})}{\partial x_i}\bigg|_{\mathbf{x}_0} \right]^2 \mathrm{Var}[X_i], \tag{22}$$

in which $\mathrm{Var}[X_i]$ is the variance of the density of input i. Thus, one possible global sensitivity measure of the importance of the uncertain input i on the variance of the model output $\mathrm{Var}[Y]$ using the approximation of equation (22) is the following:

$$\hat{S}_i^L = \frac{\left[\frac{\partial f(\boldsymbol{x})}{\partial x_i}\Big|_{\mathbf{x}_0} \right]^2 \mathrm{Var}[X_i]}{\mathrm{Var}_L[Y]}. \tag{23}$$

The output distribution of Y can be roughly approximated as a normal distribution by the first two approximate moments (equations 20 and 21). However, this is a first-order approximation and it degenerates fast with increasing nonlinearity in the model. Therefore, assessing the importance of an input variable using $\hat{S}_i^L$ can lead to misleading or unsatisfactory results if the model is nonlinear. MC simulations can help verify the quality of the approximation obtained by the delta method.

Seismic-Hazard Computation: PSHA

The goal of seismic-hazard analysis is the estimation of ground-shaking hazard due to expected future earthquakes at a site of interest. This is currently done by means of PSHA. Ground-shaking hazard is computed in terms of hazard curves, giving the annual rate of exceedance $\nu(a)$ with respect to various levels of a selected ground-motion intensity measure a. Ground-motion measures that are of engineering interest and therefore often used in PSHA are peak ground acceleration or response spectral acceleration, the latter representing the maximum response in terms of acceleration of a damped (most commonly 5% of critical damping), single-degree-of-freedom (SDOF) oscillator with a natural frequency f_{osc} due to ground motion as a rough approximation of a building response.

Within PSHA, the quantification of an annual rate of exceedance $\nu(a)$ for a target level of ground motion a considers all possible earthquake scenarios affecting the site of interest by probabilistic calculations. PSHA is generally dependent upon many inputs and several modeling decisions related to the following components: (1) geometrical characterization of possible earthquake sources, (2) characterization of the seismic activity for each contributing source, and (3) models used to describe the seismic-wave propagation from the source to the site to predict the distribution of ground motions for each considered earthquake scenario. Finally, PSHA results are obtained by an integration of all possible earthquake scenarios. In this way, one accounts for aleatory uncertainties included in the computed hazard curve. To account for epistemic uncertainties (lack of knowledge), the logic-tree framework is often applied in PSHA (Kulkarni *et al.*, 1984; Scherbaum *et al.*, 2005; Bommer and Scherbaum, 2008; Bommer, 2012). Another way to account for the epistemic uncertainties involved in PSHA is the assignment of density functions to the uncertain model inputs as done in this study. In both ways, one seeks to fulfill the aim of PSHA, which is to capture the full range of possible estimates of the seismic hazard at a site (United States Nuclear Regulatory Commission, 2012). After including the epistemic uncertainties, one obtains a distribution of hazard curves equivalent to a distribution of annual rates of exceedance for each target level a of a ground-motion measure. A thorough and comprehensive description of the underlying procedure of PSHA, including the assessment of aleatory and epistemic uncertainty, is given by the Senior Seismic Hazard Advisory Committee (Budnitz *et al.*, 1997) report, a standard reference for PSHA and in, for example, McGuire (2004).

Considering the existence of $i = 1, \ldots, m$ seismic sources, which can affect the site of interest, the total annual rate of exceedance $\nu_t(a)$ for a target ground-motion level a is the sum of the individual annual rates of exceedance $\nu_i(a)$ of each contributing source:

$$\nu_t(a) = \sum_{i=1}^{m} \nu_i(a). \tag{24}$$

For simplicity and transparency, we restrict ourselves to a single area source, emphasizing that the suggested SA method also works for the general case.

In the following, capital letters denote random variables and their lower case equivalents refer to realizations of these

random variables. Mathematically, PSHA of a single area source considering spectral acceleration as ground-motion parameter denoted as a can be expressed as

$$\nu(a,\boldsymbol{\theta},f_{\mathrm{osc}}) = \lambda_{m_{\mathrm{min}}}(\boldsymbol{\theta}_\lambda)\int_{r_L}^{r_U}\int_{m_{\mathrm{min}}}^{m_{\mathrm{max}}} f_M(m,\boldsymbol{\theta}_{f_M}) f_R(r,\boldsymbol{\theta}_{f_R}) \times \Pr(A > a|m,r,\boldsymbol{\theta}_g,s_g,f_{\mathrm{osc}})dmdr \qquad (25)$$

(e.g., Kramer, 1996; McGuire, 2004), in which $\nu(a,\boldsymbol{\theta},f_{\mathrm{osc}})$ is the annual rate of exceedance of the target level of ground motion a for an oscillator frequency f_{osc} (structural natural frequency), $\Pr(A > a|m,r,\boldsymbol{\theta}_g,s_g,f_{\mathrm{osc}})$ is the conditional probability that generated ground motion A at the site of interest exceeds the target level a for a given magnitude m, distance r, standard deviation of the logarithmic ground motion s_g, f_{osc}, and $\boldsymbol{\theta}_g$; the vectors $\boldsymbol{\theta}_\lambda$, $\boldsymbol{\theta}_{f_M}$, $\boldsymbol{\theta}_{f_R}$, and $\boldsymbol{\theta}_g$ include the parameters required to define $\lambda_{m_{\mathrm{min}}}$, f_M, f_R, and $g(.)$, respectively, and $\boldsymbol{\theta} = [\boldsymbol{\theta}_\lambda,\boldsymbol{\theta}_{f_M},\boldsymbol{\theta}_{f_R},\boldsymbol{\theta}_g,s_g]$ comprises all inputs of the seismic-hazard model; $\lambda_{m_{\mathrm{min}}}$ is the annual activity rate of the area source (number of earthquakes per year having a magnitude m larger than a minimum magnitude m_{min} considered); f_M and f_R are the probability density functions of possible earthquake magnitudes M and source-to-site distances R, respectively; upper and lower bounds of f_M are m_{max}, m_{min} and of f_R are r_U, r_L, respectively; and $g(.)$ is a function that models the mean logarithmic ground motion. For simplicity, we are ignoring finite-fault effects and we are assuming independence of f_M and f_R.

The probability that a is exceeded is given by

$$\begin{aligned}\Pr(A > a|m,r,\boldsymbol{\theta}_g,s_g,f_{\mathrm{osc}}) &= 1-\Phi\left[\frac{1}{s_g}(\ln(a)-\ln(g(m,r,\boldsymbol{\theta}_g,f_{\mathrm{osc}})))\right]\\ &= \Phi\left[\frac{1}{s_g}\ln\frac{g(m,r,\boldsymbol{\theta}_g,f_{\mathrm{osc}})}{a}\right],\end{aligned} \qquad (26)$$

in which $\Phi(\cdot)$ is the cumulative distribution function of the standard normal distribution $N(0,1)$. Ground shaking at the site of interest is modeled as lognormally distributed random variable A with $\ln A \sim N(g,s_g^2)$ having the parameters g and s_g, in which $g = g(m,r,\boldsymbol{\theta}_g,f_{\mathrm{osc}})$ and s_g is often treated as a constant across earthquake scenarios. The parameters g and s_g are provided by ground-motion models, usually empirically derived ground-motion prediction equations (GMPEs) (which have, in general, a rather simple functional form). In our study, we employ a more complex simulation-based ground-motion model representing an implementation of the stochastic method using random-vibration theory (Boore, 2003) to predict $g(m,r,\boldsymbol{\theta}_g,f_{\mathrm{osc}})$. The stochastic simulation method is a tool often used in seismic hazard analysis for low seismicity regions, which do not have enough recorded data to derive empirical GMPEs (Atkinson and Boore, 2006; Douglas *et al.*, 2013; Edwards and Fah, 2013; Rietbrock *et al.*, 2013; Bora *et al.*, 2015; Drouet and Cotton, 2015; Yenier and Atkinson, 2015). We apply the stochastic spectrum simulation as described in Molkenthin *et al.* (2014), which is based on simple duration models (Boore, 2003), Brune's source model (Brune, 1970, 1971), a stress parameter $\Delta\sigma$, path and site attenuation filters (the latter two modeled by geometrical spreading $1/R^\eta$, a frequency-depending quality factor $q(f) = q_0 f^{\alpha_q}$ and a site-specific κ_0), and the generic rock-site amplification with controlling parameter V_{S30}, the average shear-wave velocity of the upper 30 m (Boore and Joyner, 1997; Cotton *et al.*, 2006). The required seismological inputs to predict g are included in the vector $\boldsymbol{\theta}_g = [\Delta\sigma,\eta,q_0,\alpha_q,\kappa_0,V_{S30}]$.

The geometrical characterization of the contributing area source is as follows: consider a disk with radius r_{max} at depth h beneath the site of interest. The disk is parallel to the plain earth surface and its center is situated directly below the site. Hence, the shortest source-to-site distance is h and the longest is $r_0 = \sqrt{h^2 + r_{\mathrm{max}}^2}$. Assuming that earthquake hypocenters are uniformly distributed (uniformly distributed point sources) over the area source zone and after some algebraic manipulations (change of variables), the density function of source-to-site distances f_R can be derived analytically for the given geometry:

$$f_R(r,\boldsymbol{\theta}_{f_R}) = 2r/r_{\mathrm{max}}^2 \qquad (27)$$

(Ordaz, 2004). The lower bound of f_R is h and the upper bound is $r_0 = \sqrt{h^2 + r_{\mathrm{max}}^2}$. The inputs required to define f_R are therefore $\boldsymbol{\theta}_{f_R} = [h, r_{\mathrm{max}}]$.

To characterize the seismic activity of the area source, we use the doubly truncated Gutenberg–Richter (GR) relation (a doubly truncated exponential distribution). Correspondingly, the density function of earthquake magnitudes f_M is as follows:

$$f_M(m,\boldsymbol{\theta}_{f_M}) = \frac{1}{K}\beta\exp(-\beta(m-m_{\mathrm{min}})), \qquad (28)$$

in which $K = 1-\exp(-\beta(m_{\mathrm{max}}-m_{\mathrm{min}}))$ and $\beta = \ln(10)b_{\mathrm{GR}}$ with b_{GR} the exponential decay rate of the traditional GR relation, which defines the number N of earthquakes of magnitude m or greater per unit time as $N(\geq m) = 10^{a_{\mathrm{GR}}}10^{-b_{\mathrm{GR}}m}$. The lower bound of the truncation is m_{min} and the upper bound is m_{max}, referring to the minimum magnitude of interest (having a damaging potential) and the maximum expected magnitude for the considered area source, respectively. The vector comprising all required inputs defining f_M is $\boldsymbol{\theta}_{f_M} = [\beta, m_{\mathrm{min}}, m_{\mathrm{max}}]$. The seismic activity rate of the source can be expressed as $\lambda_{m_{\mathrm{min}}}(\boldsymbol{\theta}_\lambda) = \exp(\alpha-\beta m_{\mathrm{min}})$ with $\alpha = \ln(10)a_{\mathrm{GR}}$ and a_{GR} corresponds to the traditional GR relation (number of earthquakes per unit time with $m \geq 0$ is $10^{a_{\mathrm{GR}}} = \exp(\alpha)$) and $\boldsymbol{\theta}_\lambda = [\alpha, m_{\mathrm{min}}]$. Following a classical Cornell–McGuire approach, we assume that the occurrence of earthquakes in time is random and can be modeled as a Poisson process. Hence, the probability Pr that a ground-motion level a will be exceeded in time interval t is

$$\Pr(A > a,t) = 1-\exp(-\nu t), \qquad (29)$$

in which ν is the mean rate of the Poisson process, which is in our case (single area source) ν of equation (25).

The inclusion of epistemic uncertainty into the seismic-hazard model (within PSHA) leads to a distributed output of annual rates of exceedance for a certain level of a ground-motion parameter or correspondingly to a distribution A^* of ground-motion levels for a given fixed annual rate of exceedance ν_0 (e.g., $\nu_0 = 1/T_0 = 1/475$, 1/2475, or 1/10,000). Principal outputs of PSHA as shaking maps or uniform hazard spectra (UHS) are given for the mean, median, and various quantiles (percentiles) of A^* (Douglas, Ulrich, *et al.*, 2014). Therefore, the quantity of interest (model output) for the global sensitivity study is A^*, which refers to the expected distribution of ground motions (levels) for a given annual rate of exceedance ν_0 or return period $T_0 = 1/\nu_0$ induced by epistemic uncertainty. In which a^* (single realization of A^*) is the solution of the following equation:

$$\nu_0 = \nu(a, \boldsymbol{\theta}, f_{\mathrm{osc}}), \tag{30}$$

where $\boldsymbol{\theta}$, f_{osc}, and ν_0 are fixed. We obtained the values of a^* (for different $\boldsymbol{\theta}$, f_{osc}, ν_0 combinations) iteratively by solving the equivalent problem $0 = \nu(a, \boldsymbol{\theta}, f_{\mathrm{osc}}) - \nu_0$ using Newton's method. This is one possibility to compute a^*; usually a^* is derived by interpolation of the hazard curve. Epistemic uncertainty is introduced to the seismic-hazard model in such a way that $\boldsymbol{\theta} = [\theta_1, \theta_2, \ldots, \theta_k]$ is a realization of $\boldsymbol{\Theta} = [\Theta_1, \Theta_2, \ldots, \Theta_k]$, which represents a vector of random variables comprising the marginal distributions of all k uncertain inputs of the analysis.

PSHA is usually implemented in complex computer programs considering many contributing seismic sources. In addition, the complexity of the hazard integral is primarily due to the computation of the mean value of the logarithmic ground motion $g(m, r, \boldsymbol{\theta}_g, f_{\mathrm{osc}})$. As previously suggested, in practice $g(m, r, \boldsymbol{\theta}_g, f_{\mathrm{osc}})$ can be described by GMPEs with simple algebraic forms. Alternatively, however, it can be represented as a complicated, extensive computer code; for example, in FORTRAN or C, which encapsulates a ground-motion simulation technique (in our case, the stochastic ground-motion simulation technique). Our approach of SA relying on AD is suited to this situation and in principle complex computer codes pose no limitation.

PSHA of an Area Source Using Stochastic Ground-Motion Simulations: GSA

To demonstrate the proposed method of derivative-based GSA, we give an example. Let us consider a PSHA of an area source using ground-motion simulations as described in the previous section. In a first stage (1) we compute local sensitivities to understand how small changes in the inputs influence the model response locally. In a second stage (2) we present a simple graphical technique (scatter plots) to approach global sensitivities, in particular the main effects, of the inputs involved in the PSHA. In the third and fourth stages, results of our proposed derivative-based GSA method for PSHA are presented: (3) global upper bounds for the sensitivities of each input (i.e., total effect), which allow us to identify noninfluential inputs as well as rank inputs according to their influence, and (4) simple delta method GSA measures.

Our analysis includes comparisons with variance-based GSA (Sobol' method), which is often taken as a reference method. To enable those comparisons, we calculate related indexes S_{Ti} (total effect of each distributed input, equation 9) and S_i (main effect for each distributed input, equation 7). Derivative-based SA, as suggested here, requires the partial derivatives that are derived using AD.

The SA is performed for the model output $A^*(\nu_0, f_{\mathrm{osc}}, \boldsymbol{\Theta})$, which is a distribution of ground-motion levels (spectral acceleration of an SDOF system with a critical damping of 5%) for a given annual rate of exceedance ν_0 (or equivalently expressed for a return period $T_0 = 1/\nu_0$) and oscillator frequency f_{osc}. The distribution of A^* is induced by uncertain model inputs $\boldsymbol{\Theta}$. The SA of A^* is thoroughly carried out for nine cases of combinations of T_0 and f_{osc}. We consider return periods $T_0 = 1/\nu_0$ of 475 (10% of exceedance in 50 yrs, $\nu_0 = 1/475 = 2.1 \times 10^{-3}$), 2475 (2% of exceedance in 50 yrs, $\nu_0 = 1/2475 = 4.0 \times 10^{-4}$), and 10,000 yrs (0.5% of exceedance in 50 yrs, $\nu_0 = 1/10,000 = 1.0 \times 10^{-4}$), and oscillator frequencies $f_{\mathrm{osc}} = 0.5$, 10, and 100 Hz. The selected return periods are of particular interest in seismic-hazard studies, the first two return periods correspond to values typically considered for conventional buildings, as for example taken as reference for shaking maps, whereas the last return period is typically a target value for critical facilities (e.g., dams).

We consider $k = 12$ uncertain inputs (epistemic uncertainty) modeled as random variables $\boldsymbol{\Theta}$. A characterization of these uncertain inputs of the PSHA, assigned density functions and input values of the considered base case are summarized in Table 3 and are depicted in Figure 1. A single realization of the input random variables is represented by $\boldsymbol{\theta} = [\alpha, \beta, m_{\min}, m_{\max}, \Delta\sigma, \eta, q_0, \alpha_q, \kappa_0, V_{S30}, s_g, h]$. To describe the uncertainties in our synthetic example, we choose input density functions that are overall consistent with what can be expected in a stable continental tectonic setting (stable continental regions, continental crust) in Europe. The characterization of the uncertain seismological parameters $(\Delta\sigma, \eta, q_0, \alpha_q, \kappa_0, V_{S30})$ corresponds to recently obtained results of Drouet and Cotton (2015). We also considered general results related to the uncertainty of the stress parameter of Cotton *et al.* (2013). The assigned density function of s_g is consistent with typically retrieved values for Europe (Douglas, Akkar, *et al.*, 2014). The choice of seismicity parameters is guided by the values for southern Germany. To avoid physically infeasible input values, we use truncated input distributions in accordance with Table 3. The maximum extension $r_{\max}$ of the circular area source (with investigated site at the center as outlined in the previous section) is fixed to 30 km.

Results of the PSHA in terms of hazard curves $\nu(a, \boldsymbol{\theta}_0, f_{\mathrm{osc}})$ are depicted for the base case $\boldsymbol{\theta}_0$ in Figure 2. Hazard curves are shown for the three different f_{osc} (0.5, 10, and 100 Hz) of interest in the SA. Return periods (475, 2475,

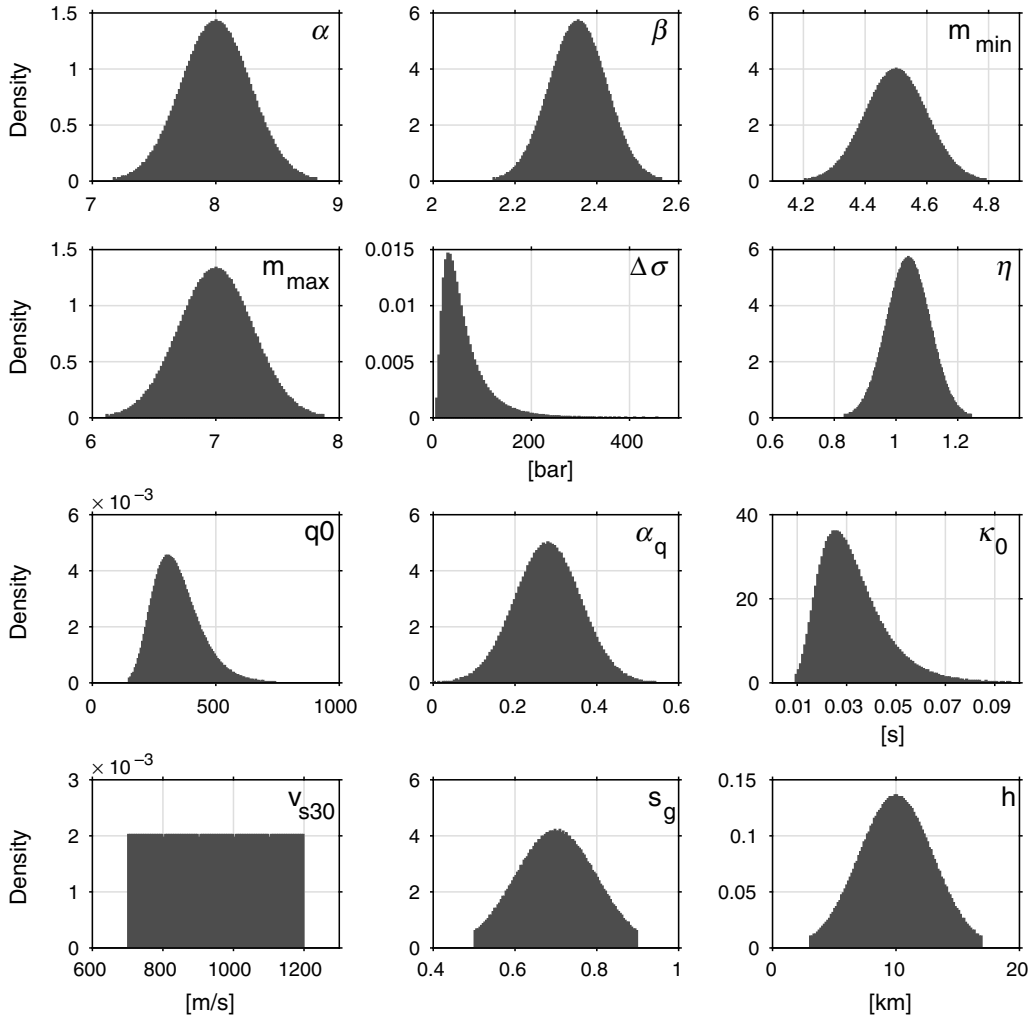

Figure 1. Characterization of the epistemic uncertainty: normalized histograms of the uncertain input parameters.

Table 3
Characterization of the Epistemic Uncertainty: Density Functions Assigned to the Input Parameters

Number	Input Parameter	Input Group	Base Case	Density Function	Support
1	Annual activity level of Gutenberg–Richter relation, α	Seismicity	8.0	$\mathcal{N}(8.0, 0.28^2)$	(7.169, 8.831)
2	Exponential decay rate of Gutenberg–Richter relation, β	Seismicity	2.354	$\mathcal{N}(2.354, 0.07^2)$	(2.146, 2.562)
3	Minimum magnitude (lower bound of truncation), $m_{\min}$	Seismicity	4.5	$\mathcal{N}(4.5, 0.1^2)$	(4.203, 4.797)
4	Maximum magnitude (upper bound of truncation), $m_{\max}$	Seismicity	7.0	$\mathcal{N}(7.0, 0.3^2)$	(6.110, 7.890)
5	Stress parameter, $\Delta\sigma$ [bar]	Ground-motion simulation	50.0	$\ln\mathcal{N}(3.912, 0.69078^2)$	(5, 500)
6	Exponent of the geometrical spreading, η	Ground-motion simulation	1.04	$\mathcal{N}(1.04, 0.07^2)$	(0.832, 1.248)
7	Path attenuation quality factor $q(f) = q_0 f^{\alpha_q}$, q_0	Ground-motion simulation	331.13	$\ln\mathcal{N}(5.8025, 0.27631^2)$	(145.838, 751.845)
8	Path attenuation quality factor $q(f) = q_0 f^{\alpha_q}$, α_q	Ground-motion simulation	0.28	$\mathcal{N}(0.28, 0.08^2)$	(0, 0.560)
9	Site attenuation, κ_0 [s]	Ground-motion simulation	0.03	$\ln\mathcal{N}(\ln(0.03), 0.4^2)$	(0.009, 0.098)
10	Site amplification, Generic rock site, V_{S30} [m/s]	Ground-motion simulation	950.0	$\mathcal{U}(700, 1200)$	(700, 1200)
11	Standard deviation of the logarithmic ground motions, s_g	Ground-motion simulation	0.7	$\mathcal{N}(0.7, 0.1^2)$	(0.5, 0.9)
12	Depth of the source, h [km]	Geometrical characterization	10.0	$\mathcal{N}(10, 3^2)$	(3, 17)

$\mathcal{N}(\cdot)$, normal distribution; $\ln\mathcal{N}(\cdot)$, lognormal distribution; $\mathcal{U}(\cdot)$, uniform distribution.

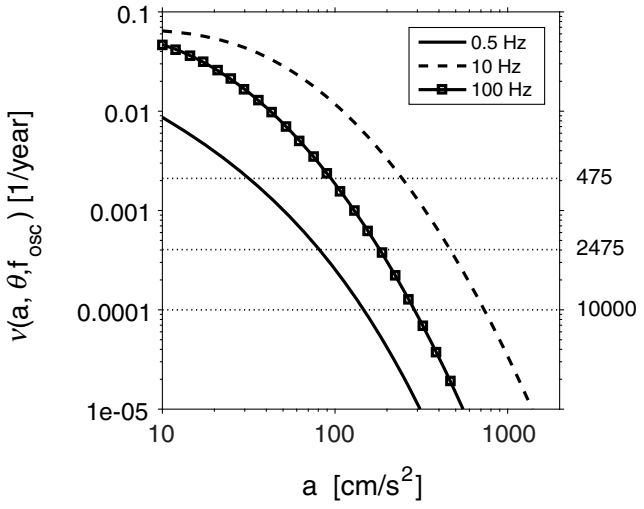

Figure 2. Hazard curves for different oscillator frequencies (f_{osc}) for the base case. Horizontal dotted lines indicate different return periods ($T_0 = 1/\nu_0 = 475$, 2475, and 10,000 yrs).

and 10,000 yrs), which are considered in the SA, are marked as horizontal lines in the figure. The base case parameterization $\boldsymbol{\theta}_0$ is given in Table 3.

The distribution of A^*, induced by epistemic uncertainty, is obtained by evaluating the model at N sample points $\boldsymbol{\theta}_j$ with $j = 1, 2, \ldots, N$ solving iteratively equation (30) using Newton's method. The N evaluations are done for all cases considered (combinations of $T_0 = 1/\nu_0$ and f_{osc} mentioned above). Resulting distributions of A^* in the N model evaluations are depicted in terms of normalized histograms in Figure 3. As expected with increasing return period T_0 (decreasing ν_0), A^* shifts to larger ground-motion levels. Moreover, we observe from Figure 3 that the distribution of the model output A^*, for a given annual rate of exceedance ν_0 (or return period $T_0 = 1/\nu_0$) and fixed f_{osc}, is approximately lognormally distributed:

$$\ln(A^*) = Y \sim \mathcal{N}(\mu, \sigma^2). \tag{31}$$

This is indicated by the maximum-likelihood fitted lognormal density functions (dashed black line in Fig. 3).

Local Sensitivities

To assess how small changes in the inputs influence the model response, we compute local sensitivities at a reference point $\boldsymbol{\theta}_0$ (Table 3). The model output is $a^*(\nu_0, f_{\text{osc}}, \boldsymbol{\theta})$, the solution of equation (30); see also equation (25). Consequently, local sensitivities are computed as follows:

$$\begin{aligned} d_i &= \left.\frac{\partial a^*(\boldsymbol{\theta})}{\partial \theta_i}\right|_{\boldsymbol{\theta}_0} \\ &= -\frac{\partial \nu(a, f_{\text{osc}}, \boldsymbol{\theta})}{\partial \theta_i} \left(\frac{\partial \nu(a, f_{\text{osc}}, \boldsymbol{\theta})}{\partial a}\right)^{-1} \Bigg|_{a^*(\boldsymbol{\theta}_0)}. \end{aligned} \tag{32}$$

Relative sensitivities $d_i^{\text{rel}} = d_i(\frac{\theta_i}{a^*(\boldsymbol{\theta}_0)})$ of a^* with respect to each input θ_i are shown in Figure 4. A percentage change in the inputs (e.g., +1%) is related to a percentage change in the model response. One can observe both the direction and magnitude of the relative change in the model response due to small relative changes in the individual inputs. For example, we see that an increase in α leads to an increase in a^*, whereas an increase of η causes a decrease in a^*. If the stress parameter $\Delta\sigma$ is increasing by 5% then the level of expected ground motion a^* at 100 Hz and 475 yr return period is increasing by ≈4%. We clearly see which inputs are correlated and which are anticorrelated with the model response, regardless of oscillator frequency f_{osc} or return period T_0. The group of correlated inputs includes $\alpha, m_{\max}, \Delta\sigma, q_0, \alpha_q, s_g$, and the group of anticorrelated inputs includes $\beta, m_{\min}, \eta, \kappa_0, V_{S30}, h$. We note that even though in certain frequency return period cases some input variables (e.g., see κ_0) may show practically zero correlation, they never change their correlation sign.

The absolute magnitude of the relative sensitivities in Figure 4 allows us to identify the inputs with the highest local effect on the model response. Inputs are varied by the same small relative change from the base case. Independently of f_{osc} and T_0, we find that there are three important inputs, namely the seismicity parameters β, α and ground-motion prediction parameter η. Among these three, β has the largest effect. For a low $f_{\text{osc}} = 0.5$ Hz, the effect of α is stronger than that of η, whereas the effect of η is slightly larger than that of α for larger f_{osc} and T_0. In general, it seems that the effect of the seismicity parameters is more pronounced for low f_{osc}. There is a fourth input that has a substantial influence on the model response. For large f_{osc}, it is ground-motion prediction parameter s_g, whereas for low f_{osc} (0.5 Hz) it is seismicity parameter $m_{\max}$. The input $m_{\max}$ has significant influence at low f_{osc} and its effect on the model response increases in general, with larger return periods T_0. The input $\Delta\sigma$ always has a moderate effect on the model response, regardless of f_{osc} or T_0. The influence of κ_0 increases strongly with larger f_{osc}. For large f_{osc} and all T_0, the effect of κ_0 is moderate and the absolute magnitude of its relative sensitivities is comparable with those of $\Delta\sigma$ and larger than those of h and V_{S30}. Inputs with negligible effect on the model response are q_0, α_q and for low f_{osc} also κ_0. The input $m_{\min}$ has a negligible influence in general, except for low return periods T_0 and large f_{osc}. In this case, one can observe a minimal to moderate effect of $m_{\min}$ on the model output.

Analysis of local perturbations may be valuable under certain circumstances; however, often one is interested in the effect the uncertainty of an input has on the model response across the entire input domain. To address this issue, we perform a GSA considering the individual uncertainties in the inputs.

Global Sensitivities: Graphical Techniques, Scatter Plots

Scatter plots (Fig. 5) of model evaluations at several sample points (quasi-MC samples) can serve as a first simple

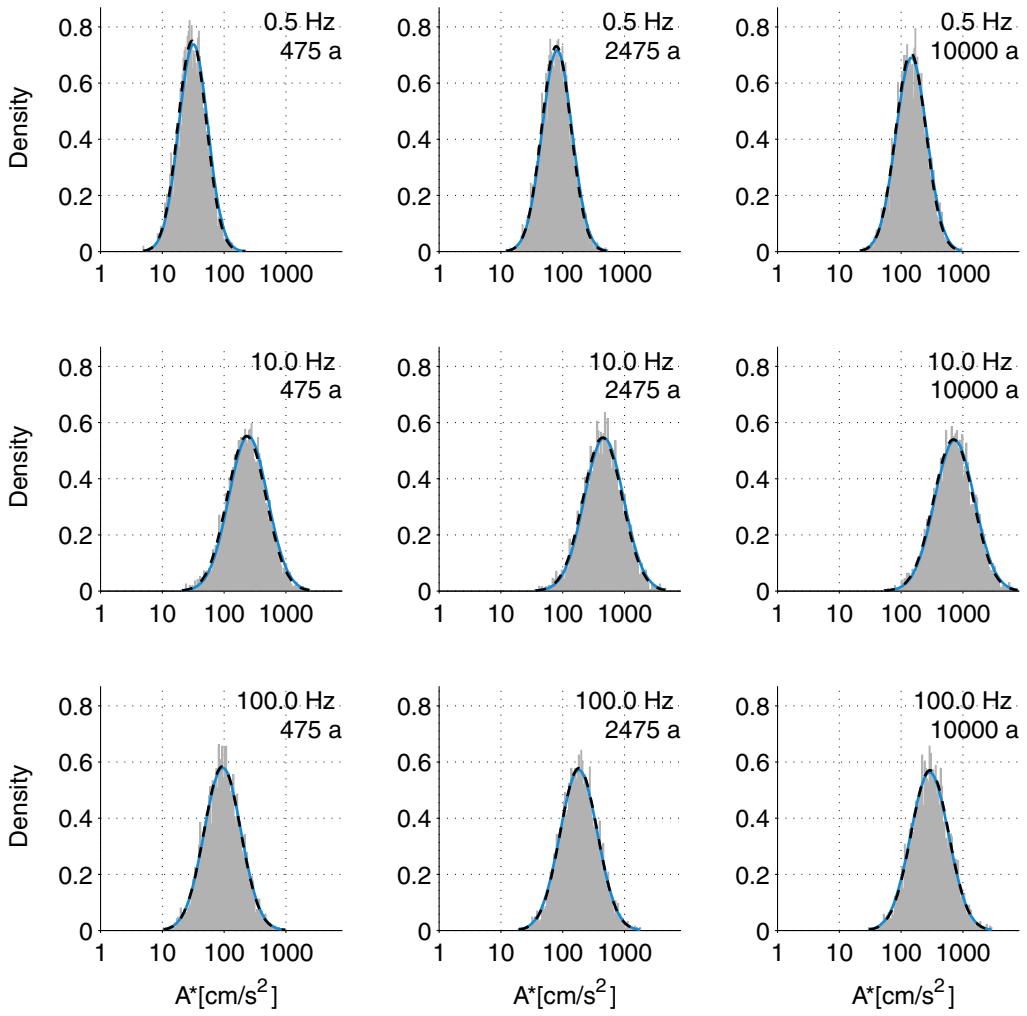

Figure 3. Distributions of ground-motion levels A^* (model output) for nine cases with different return periods ($T_0 = 1/\nu_0 = 475$, 2475, and 10,000 yrs) and different natural frequencies of a single-degree-of-freedom oscillator ($f_{\text{osc}} = 0.5$, 10, and 100 Hz). Normalized histograms (gray bars) of $N = 2^{12}$ simulations are shown for each case using quasi-Monte Carlo sampling; fitted density functions (lognormal distributions) via maximum-likelihood estimation are shown by black dashed lines; approximated density functions via delta method are shown by solid lines. The color version of this figure is available only in the electronic edition.

graphical tool for GSA to assess the importance of each of the k uncertain inputs $\Theta_1, \Theta_2, \ldots, \Theta_k$ on the model response A^*. The input points are sampled from the distribution of the inputs. An example of such scatter plots for the case ($T_0 = 475$ yrs, $f_{\text{osc}} = 100$ Hz) is depicted in Figure 5. The model output A^* (same vertical scale for all plots) is plotted against each of the 12 uncertain inputs Θ_i. The existence of some shape or pattern in the cloud of points indicates that the factor is important, whereas noninfluential inputs show a rather uniform cloud of points. To quantify the concept of shape in terms of a measure for the importance of an input, we roughly estimate the variation of the conditional expectation $\mathrm{E}[A^*|\Theta_i]$ (equation 6) in a rather simple way. We are taking averages of the model output A^* within bins of 50 points in each scatter plot, approximating $\mathrm{E}[A^*|\Theta_i]$ in each bin, depicted by a solid line in Figure 5. If $\mathrm{E}[A^*|\Theta_i]$ varies strongly for an input among the bins, then this input is supposed to be an influential or important input, whereas a constant $\mathrm{E}[A^*|\Theta_i]$ indicates that the input is noninfluential and could be fixed. The variation of $\mathrm{E}[A^*|\Theta_i]$ for each input is illustrated by box plots in Figure 6 (left). The variance of $\mathrm{E}[A^*|\Theta_i]$ is directly related to the main effect S_i of an input Θ_i (see equation 7), which we also estimated as $\widehat{S}_i$ using the previously obtained rough approximations of $\mathrm{E}[A^*|\Theta_i]$. Results are shown in Figure 6.

In Figure 5, one can recognize a pattern in the scatter plots for the uncertain ground-motion parameters $\Delta\sigma$ and κ_0. Indeed, low values of $\Delta\sigma$ have a large effect as they significantly limit the variation in the model response A^* (Fig. 5). A similar trend can be identified for large values of κ_0; that is, bounding the variation of A^* substantially. In contrast to that, the scatter plots of the uncertain inputs m_{min} and m_{max} show a rather uniform cloud and the approximation of $\mathrm{E}[A^*|\Theta_i]$ is nearly constant over the input domain (solid line in Fig. 5).

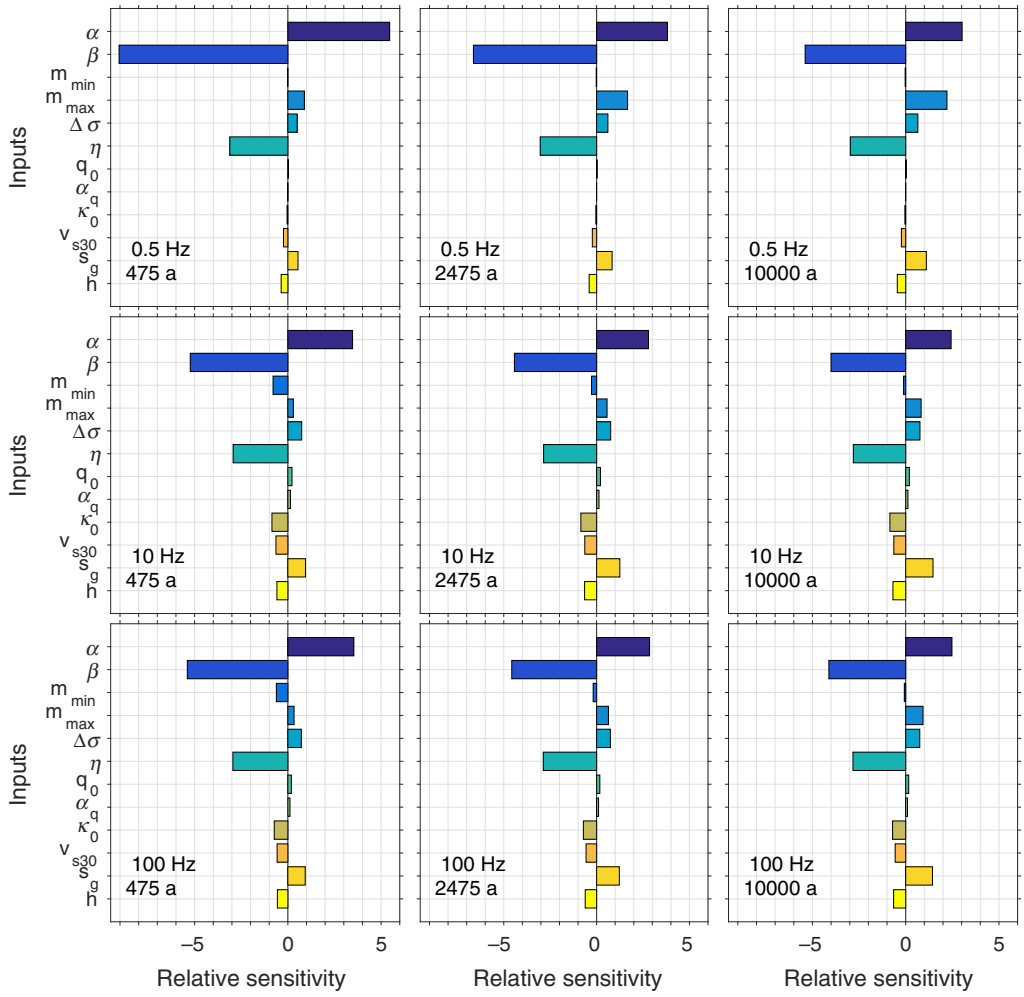

Figure 4. Local relative sensitivities with direction of the effects are shown for nine cases with different return periods ($T_0 = 1/\nu_0 = 475$, 2475, and 10,000 yrs) and different natural frequencies of a single-degree-of-freedom oscillator ($f_{\text{osc}} = 0.5$, 10, and 100 Hz). The same positive proportional change of an input parameter (+1%) is related to the corresponding proportional change of the model output a^* in percent. The color version of this figure is available only in the electronic edition.

Therefore, these inputs can be identified as noninfluential. Summaries of the variation of $\mathrm{E}[A^*|\Theta_i]$ and the approximated main effects $\widehat{S}_i$ indicate that the main influencing uncertain input factor is $\Delta\sigma$ (see Fig. 6). In addition, κ_0 has a substantial effect on the variation of the model response, and η can be identified as the third main important input (Fig. 6, right). The uncertain inputs $m_{\min}$, $m_{\max}$, q_0, and α_q have a negligible influence on the model response and could be fixed at their expectations. However, analyzing scatter plots in the case of many inputs, several return periods and intensity measures can become impractical or cumbersome. To that purpose, in the following section we present a more practical and computationally efficient approach.

Global Sensitivities: Upper Bounds for the Total Effect of Each Input

In this section, we present the suggested efficient derivative-based GSA method for PSHA to obtain global upper bounds U_i for the total effect S_{Ti} of each uncertain input Θ_i (with $i = 1, 2, \ldots, k$) on the distribution of model response A^*, as given in equation (14). The suggested method is sampling based and requires the evaluation of the model output as well as the evaluation of its gradient with respect to the inputs at each sample point. For this purpose, we apply AD. In practice, the suggested derivative-based GSA approach consists of the following five steps: (1) differentiating the computer code of the entire PSHA model including the computer code for $g(m, r, \boldsymbol{\theta}_g, f_{\text{osc}})$ and using reverse mode AD to obtain its ADM, (2) assigning a density function to each input to represent its uncertainty, (3) creating quasi-MC samples from an LDS and using inverse-sampling theorem to obtain input samples accordingly to the assigned densities, (4) solving equation (30) and subsequently evaluating the ADM at the obtained solutions and giving the gradient at all sample points, and (5) finally computing the upper bounds U_i for S_{Ti} to identify noninfluential and important uncertain inputs.

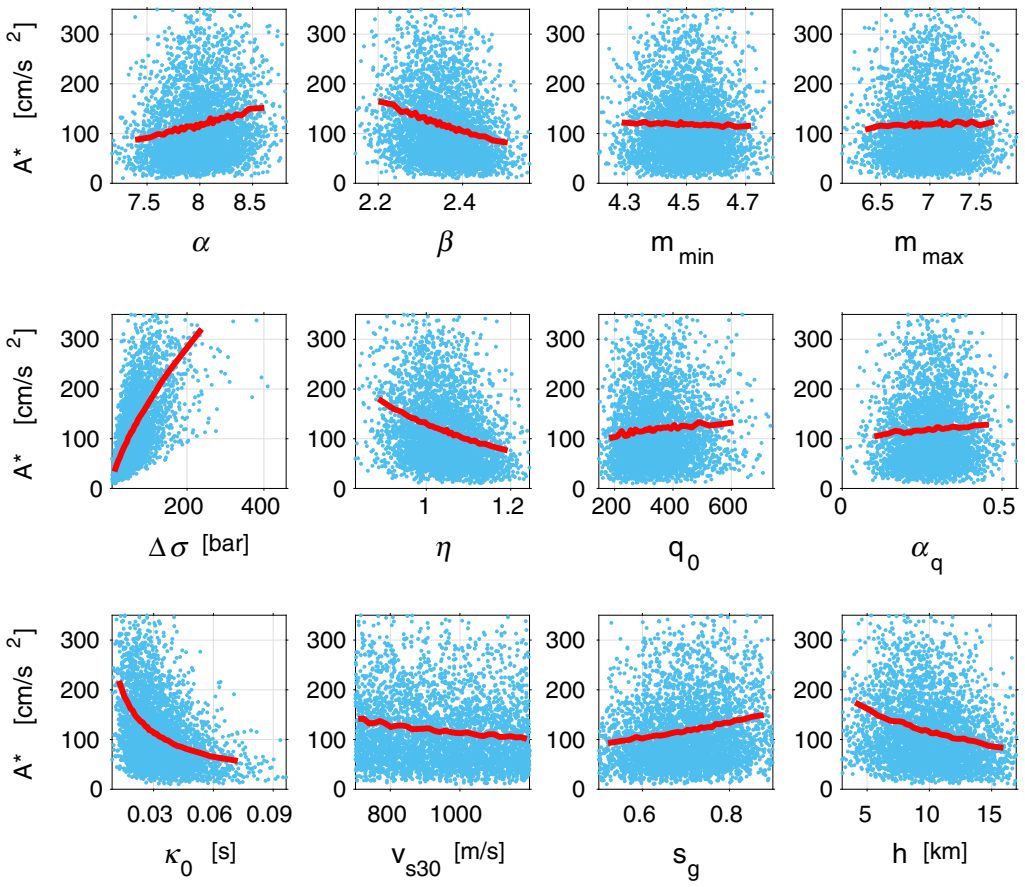

Figure 5. Scatter plots of the model output A^* versus inputs (dots) for the case $T_0 = 475$ yrs, $f_{\text{osc}} = 100$ Hz, number of quasi-Monte Carlo samples $N = 4096$. The approximated conditional expectation $\text{E}[A^*|\Theta_i]$ is depicted as solid line in each subplot. The color version of this figure is available only in the electronic edition.

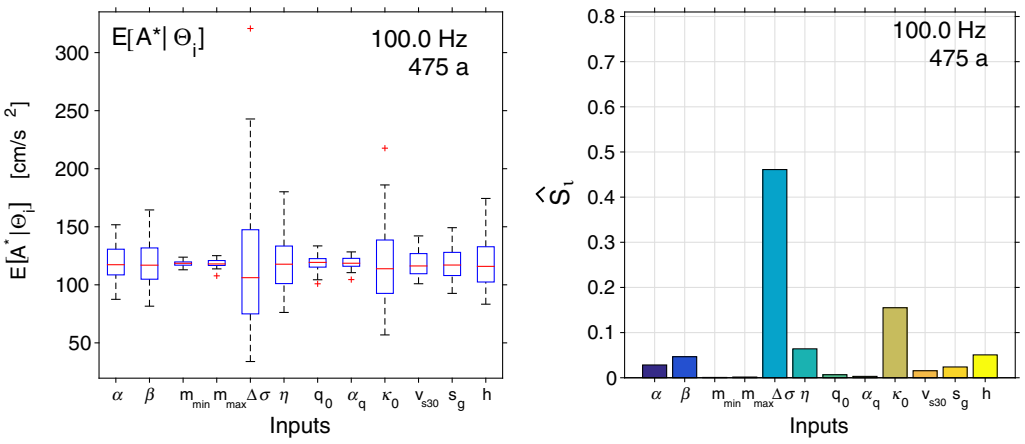

Figure 6. Estimates of global sensitivities based on a simple smoothing technique. (Left) Variation of approximated $\text{E}[A^*|\Theta_i]$, and (right) approximated main effect $\widehat{S}_i$. The color version of this figure is available only in the electronic edition.

Results (upper bounds U_i) are presented for nine different cases of T_0 and f_{osc} as dark shaded bars for each input in Figure 7. To corroborate the obtained global upper bounds U_i, we also compute the corresponding total effects S_{Ti}, light shaded bars for each input in Figure 7. The dashed vertical line depicts the value $1/k$ in Figure 7. Uncertain inputs with upper bounds U_i significantly lower than $1/k$ can be considered as noninfluential. Results obtained by the suggested method and the reference method (S_{Ti}) show a very similar picture of the effects that the individual inputs have on the

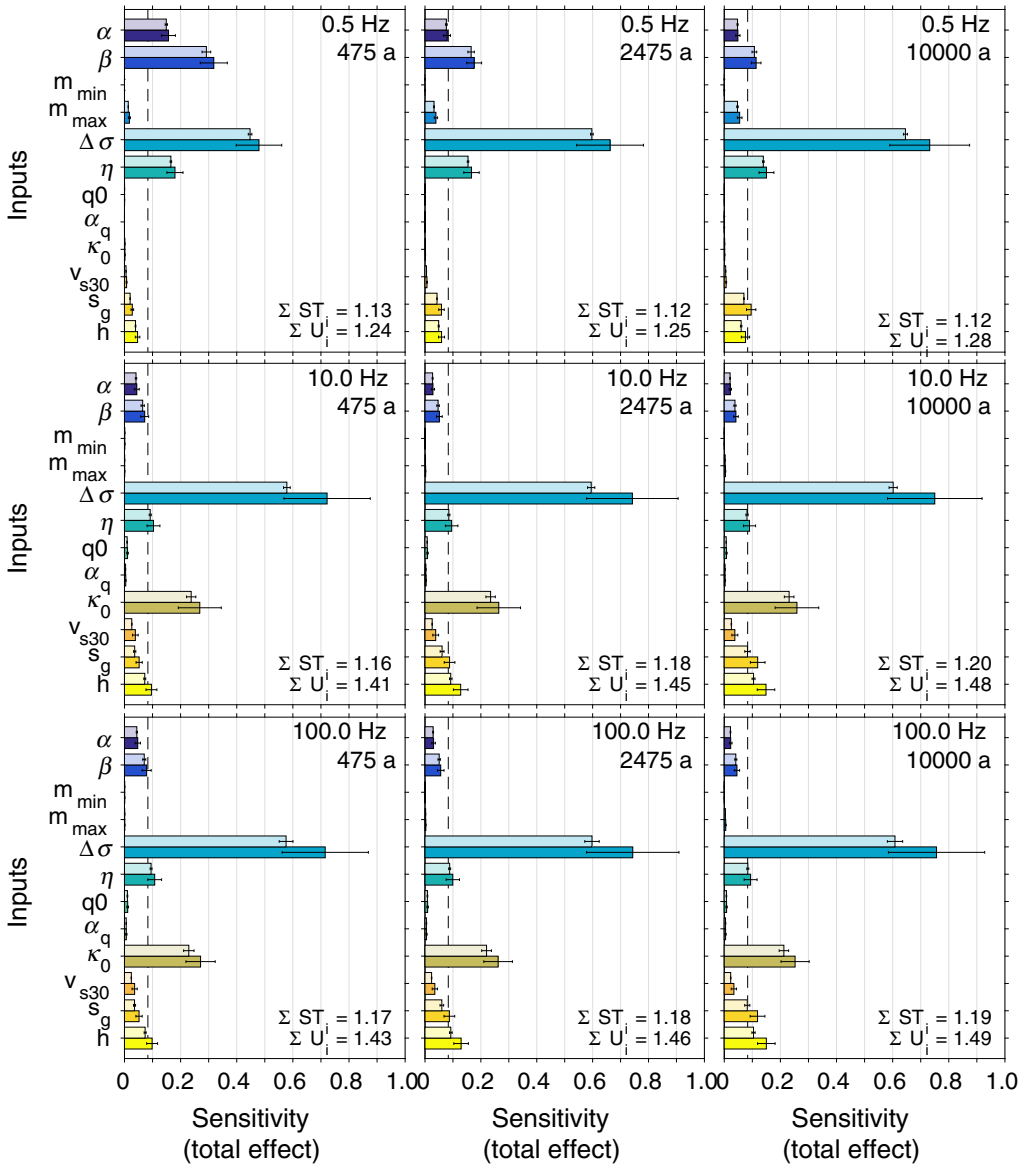

Figure 7. Global upper bounds U_i for the total effect of each uncertain input on the distributed model response A^* are shown and compared with the total global sensitivity indexes S_{T_i} for different oscillator frequencies and return periods. For each input two bars are shown, first bar (light shading) depicts S_{Ti} and second bar (dark shading) shows U_i. Sample size is $N_{U_i} = 64$ to compute U_i, whereas the sample size for the computation of S_{T_i} is $N_{S_{T_i}} = 1024$. Error bars represent the standard deviation of the estimates based on 64 (4) runs in the case of U_i (S_{Ti}). The color version of this figure is available only in the electronic edition.

uncertainty of the model response. However, we emphasize that computing the derivative-based GSA measures U_i is much cheaper for two reasons. First, the number of sample points N_{U_i} required to reliably estimate U_i is much smaller than the number of sample points $N_{S_{Ti}}$ needed to estimate S_{Ti}, as illustrated for our case in Figure 8. Mean estimates for U_i and S_{Ti} based on different numbers of samples N are shown for all uncertain inputs for the case $f_{\text{osc}} = 100$ Hz and $T_0 = 475$ yrs. Estimates for U_i converge faster, and therefore the evaluation of U_i requires only about $N_{Ui} \geq 64$ sample points, whereas in case of the total effect S_{Ti} one needs approximately $N_{S_{Ti}} \geq 1024$. Second, the final computation of the total effect S_{Ti} related to each uncertain input requires $N_{S_{Ti}}(k+2)$ (= 14,336) model evaluations, whereas for the estimation of U_i this is only about N_{Ui} (≈64). Considering the additional computational costs due to reverse mode AD, this introduces a modest multiplicative factor $c \leq 5.6$ for each model run. Hence, the calculation costs in terms of the number of model evaluations are approximately of ≈360 for U_i, which results in a gain factor of ≥40. The upper bounds U_i are quite similar to the corresponding S_{Ti} (see Fig. 7 and Table 4). In addition, main effects S_i show a similar overall picture regarding an importance ranking of the individual uncertain inputs as can be seen from Table 4 and from results of Figure 6. Therefore, an importance ranking of the effects of the different uncertain inputs based on

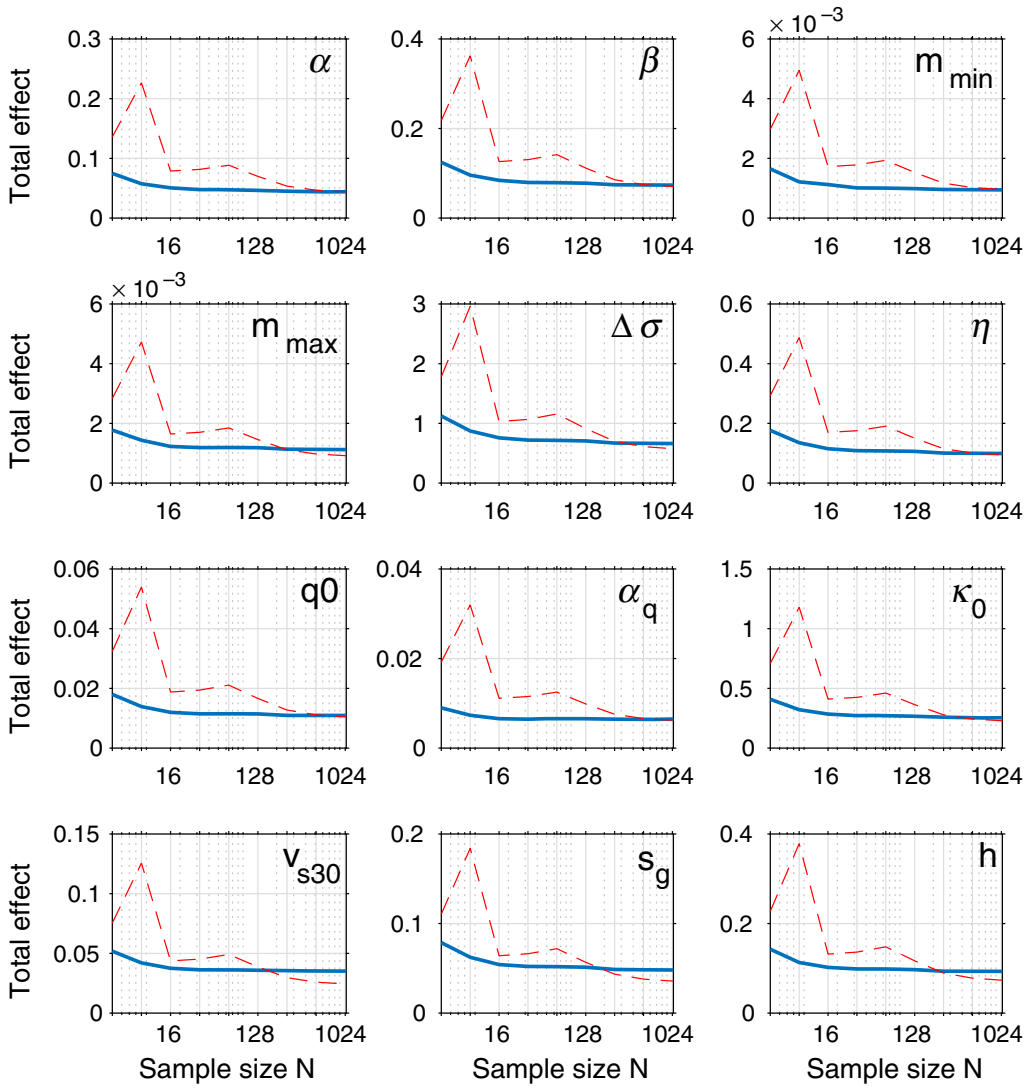

Figure 8. Sample size required to estimate U_i (solid lines) and S_{Ti} (dashed lines). The color version of this figure is available only in the electronic edition.

the upper bounds U_i is possible in the case of PSHA. Noninfluential inputs as well as important inputs considering their uncertainties can be easily identified for the different cases of interest within the PSHA as demonstrated in Figure 7. For noninfluential uncertain input parameters, it is useless to take into account variability because it has no impact on the uncertainty of the final results. For example, in this PSHA study, the following inputs can be identified as noninfluential: $m_{\min}$, q_0, and α_q regardless of oscillator frequency or return period, and also κ_0 is noninfluential for low f_{osc}. Main influencing factors for low f_{osc} are $\Delta\sigma$, β, η, and α with decreasing influence of β and α with increasing return periods. For large f_{osc} (10 or 100 Hz), the most important inputs are $\Delta\sigma$ and κ_0. Additionally, the following factors have a significant impact on the uncertainty of the model response: h, s_g, and η. The low impact of the parameters q_0 and α_q (defining the quality factor) is probably related to the fact that in the PSHA study only small distances (<35 km) occur, which is a result of the geometrical setting of the area source. The strong influence of $\Delta\sigma$ and κ_0 can be attributed to their large uncertainty and their strong influence on the spectral bandwidth, which is particularly influential in the response spectral values for high oscillator frequencies (Bora *et al.*, 2016).

At first sight, the results of GSA (Fig. 7) seem to be inconsistent with those obtained in Figure 4 (local relative sensitivities). However, a large local relative sensitivity of an input parameter does not necessarily lead to a large global sensitivity, because the uncertainty range of this input can be relatively small compared with other inputs. One can consider these two types of SA outcomes to complement each other. To estimate local relative sensitivities (Fig. 4), the same small proportional change (same relative error) for all the inputs is assumed. In contrast to that, in the example the

Table 4
Global Sensitivity Measures in the Case $T_0 = 475$ yrs and $f_{osc} = 100$ Hz for the Model Response A^* (with $N_{U_i} = 64$, $N_S = 1024$)

Input	U_i	S_{T_i}	S_i
α	0.047	0.044	0.026
β	0.079	0.070	0.038
m_{min}	0.001	0.001	0.000
m_{max}	0.001	0.001	0.000
$\Delta\sigma$	0.715	0.576	0.453
η	0.108	0.095	0.069
q_0	0.011	0.010	0.008
α_q	0.007	0.006	0.003
κ_0	0.271	0.229	0.143
V_{S30}	0.036	0.024	0.016
s_g	0.052	0.036	0.020
h	0.098	0.074	0.050
Sum	1.427	1.167	0.826

N_{U_i}, number of sample points to estimate U_i; N_S, number of sample points to estimate S_i and S_{T_i}; U_i, upper bound for the total effect; S_{T_i}, total effect; S_i, main effect.

Table 5
Global Sensitivity Measures in the Case $T_0 = 475$ yrs and $f_{osc} = 100$ Hz for the Model Response $\ln A^*$ (with $N_{U_i} = 64$, $N_S = 1024$)

Input	U_i	S_{T_i}	S_i
α	0.035	0.034	0.033
β	0.058	0.056	0.055
m_{min}	0.001	0.001	0.001
m_{max}	0.001	0.001	0.001
$\Delta\sigma$	0.537	0.528	0.527
η	0.084	0.082	0.081
q_0	0.008	0.007	0.006
α_q	0.004	0.003	0.002
κ_0	0.193	0.186	0.183
V_{S30}	0.023	0.018	0.018
s_g	0.037	0.028	0.027
h	0.066	0.059	0.058
Sum	1.046	1.003	0.993

N_{U_i}, number of sample points to estimate U_i; N_S, number of sample points to estimate S_i and S_{T_i}; U_i, upper bound for the total effect; S_{T_i}, total effect; S_i, main effect.

uncertainty range of seismicity parameters and also of the input parameter η is relatively small compared with the other inputs, especially $\Delta\sigma$ and κ_0, which have a relative large uncertainty range. If this is considered, the SA outcomes shown in Figures 4 and 7 do not disagree. However, results of local and global SA agree only for a few limited model types such as linear or nearly linear. Disagreement between the results typically reveals a nonlinear-nonmonotonic behavior of the model for one or more inputs.

If we take the log transformations of the model output A^* and correspondingly if we consider $\ln A^*$ as the model response in the analysis, we observe that the upper bounds U_i of the sensitivities with respect to each uncertain input almost coincide with their total effects S_{Ti} as depicted in Table 5. In addition, upper bounds U_i also nearly coincide with the main effects S_i of the model inputs. The sum of all U_i, S_{T_i}, and S_i, respectively, are close to one. This indicates that the seismic-hazard model with $\ln A^*$ as the output becomes quasi-additive and possibly even linear in its inputs. Note that inputs are assumed independent. The overall picture related to the identification of noninfluential and important inputs in terms of their influence on the uncertainty of the model response has not changed in the considered cases and so the above statements about the influence of the different uncertain inputs remain valid. From a practical point of view, however, the apparent approximately nearly linear behavior of the model with output $\ln A^*$ opens up the possibility to apply the delta method as described in the next section.

Global Sensitivities: Delta Method

For completeness, because we realized through GSA that the $\ln A^*$ model is basically additive and nearly linear, we now include the classical delta method approximation for this model and its derived sensitivities $\hat{S}_i^L$ as in equation (23). In the case of a nearly linear model with an approximately Gaussian output and unimodal symmetric inputs, the delta method (first-order uncertainty propagation) is a very efficient way of performing GSA and uncertainty analysis of the distributed model response using accurately computed derivatives. Main effects S_i of the uncertain inputs computed via quasi-MC simulations (Sobol' method) with $N_S = 1024$ are compared with those $\hat{S}_i^L$ obtained via the delta method, and they are presented in Figure 9. The estimates $\hat{S}_i^L$ approximated by the delta method agree well with the estimates for the main effects S_i using quasi-MC simulations in all cases. In addition, the distribution of the model response ($\ln A^*$) can be roughly approximated simultaneously, and includes possible estimations of quantiles. Results of the approximated model output distribution induced by the uncertainty of the inputs are illustrated for the nine considered cases of f_{osc} and T_0 in Figure 3. The estimated density function using the delta method (solid line) is compared with quasi-MC simulations of $N = 4096$ sample points for all in the SA considered cases. The normalized histograms of the simulations as well as the density functions (fitted, dashed line; delta method, solid line) agree well across all cases. The results (GSA estimates and uncertainty estimates) are interesting from the practical point of view of computational costs. The delta method requires only one single evaluation of the differentiated model (ADM), and therefore $N = 1$, which leads to an overall computational cost (accounting for the additional costs of the ADM) of approximately only six times that of the original model.

Finally, we consider the entire UHS of the PSHA, which refers to the distributed model response $\ln A^*$ for a whole spectrum of f_{osc} given one selected fixed return period T_0. We compute the global sensitivities $\hat{S}_i^L$ of the UHS with respect to each uncertain input using the delta method (Fig. 10, top). These results suggest that the uncertainty in the UHS

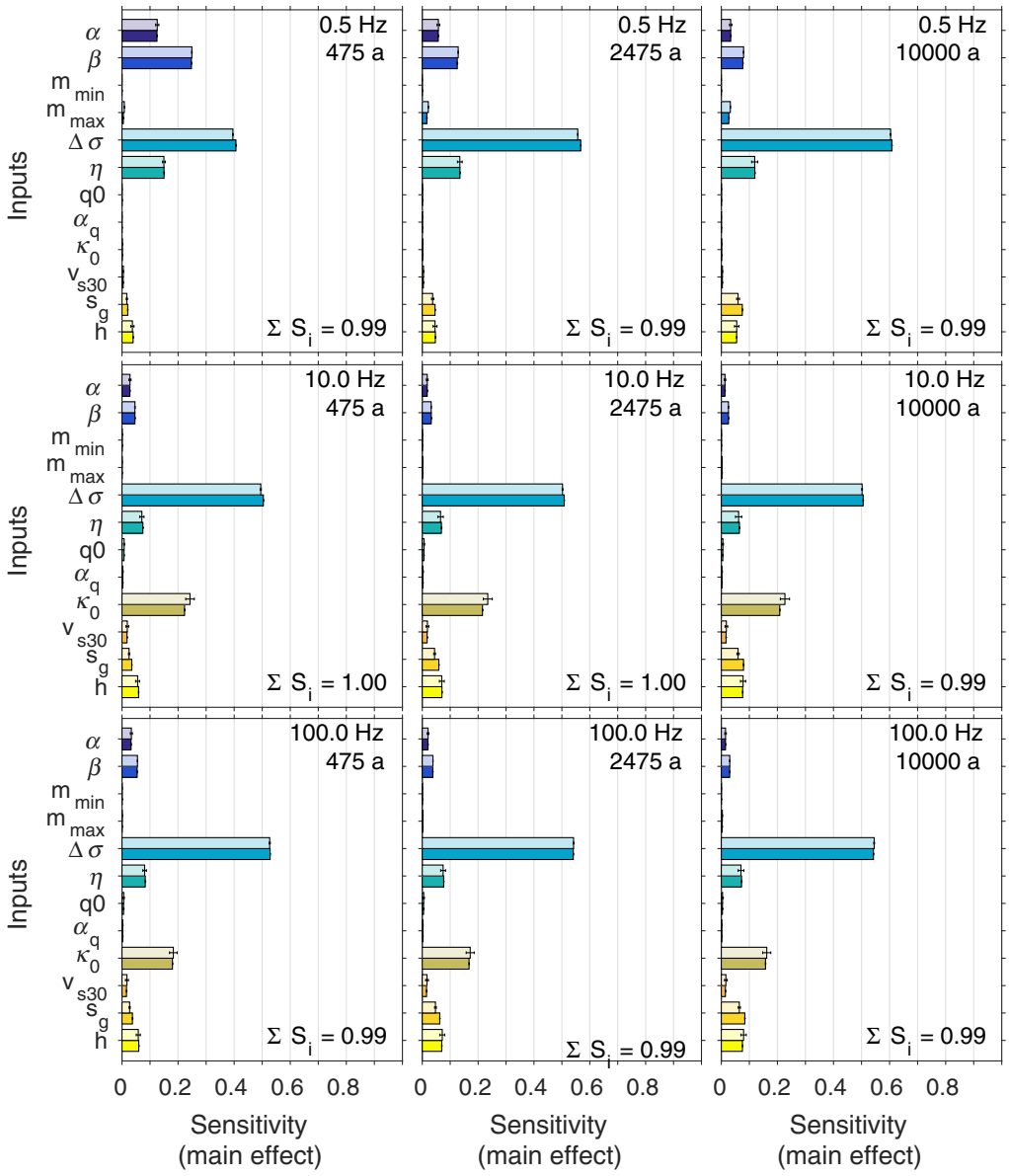

Figure 9. Comparison of main effects S_i (first, light bar for each input) with the estimated delta method global sensitivity analysis (GSA) measure $\hat{S}_i^L$ (second, dark bar for each input) for the model response $\ln A^*$. Error bars represent the standard deviation of the S_i estimates based on four runs. The color version of this figure is available only in the electronic edition.

($T_0 = 475$ yrs) is mainly due to the epistemic uncertainty in the stress parameter $\Delta\sigma$ (≈37%–63%) and for large f_{osc} (> 5 Hz) to epistemic uncertainty related to κ_0 (≈10%–42%). Other important factors introducing uncertainty in the UHS are β (≈13%–25%), η (≈13%–15%), and α (≈7%–12%) for $f_{\text{osc}} < 1$ Hz, see Figure 10 (top). The portion of the uncertainty in the UHS due to the uncertain input is given in brackets. Noninfluential inputs are $m_{\min}, m_{\max}, q_0, \alpha_q, V_{S30}$, and are not shown in the figure. In addition to the GSA estimates, we use quasi-MC simulations to compute different quantiles of the UHS and we compare these with estimates of the quantiles simply obtained by the delta method. The computational cost for quasi-MC simulations is $N = 4096$ for each considered f_{osc} whereas for the delta method this is $N = 1$. Results for a return period of $T_0 = 475$ yrs and oscillator frequencies f_{osc} from 0.5 to 100 Hz are depicted in Figure 10 (bottom). The quantiles of the UHS estimated via the delta method agree approximately with those derived from quasi-MC simulations (see Fig. 10, bottom). For low f_{osc} up to 5 Hz and for large $f_{\text{osc}} > 60$ Hz, estimates of the delta method and those of the quasi-MC simulations nearly coincide, whereas for the frequency band $5 \text{ Hz} \leq f_{\text{osc}} \leq 60$ Hz the delta method mostly overpredicts the quantiles and the mean by an amount up to 15%.

Conclusions

SA plays a key role in PSHA for the model building, as well as for the evaluation and communication of the obtained

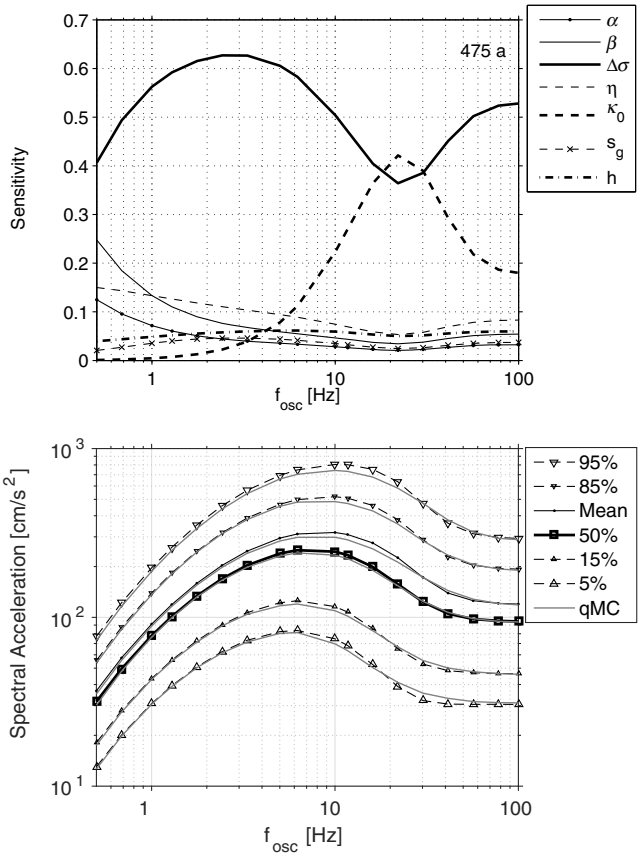

Figure 10. (Top) Approximated global sensitivities $\hat{S}_i^L$ (delta method GSA measure) of the uniform hazard spectrum (UHS of return period $T_0 = 475$ yrs) for influential uncertain inputs. (Bottom) Corresponding mean UHS and estimated quantiles using delta method (black lines with markers), and quasi-Monte Carlo estimates (qMC) of the quantiles (solid gray shaded lines without markers) with sample size $N = 4096$ for each considered oscillator frequency f_{osc} in the UHS.

results. In this study, we proposed derivative-based GSA methods using AD. These methods have the advantage that they remain computationally feasible also for complex models. AD enables the efficient and accurate computation of the required derivatives. Upper bounds for global sensitivities; that is, for the total effect of each uncertain input to the PSHA, can be easily obtained with low computational costs compared with classical variance-based methods, as they require far fewer model evaluations. To the best of our knowledge, it is the first time that a derivative-based GSA using upper bounding of the global input sensitivities is combined with the power of AD in practice. In addition, we observed that for the log-transformed model response (ground-motion levels given a return period), the seismic-hazard model becomes nearly linear. Therefore, global sensitivities with respect to the uncertain inputs can be estimated satisfactorily with a first-order uncertainty propagation; that is, the delta method. The distribution of the model response can be roughly approximated simultaneously. The computational effort of this second, derivative-based method combined with AD is minimal, which means it has the cost of the model evaluation times a small constant, independent of the number of inputs. However, one has to keep in mind that the delta method as applied here is only a first-order approximation and gives feasible results only in the case of a nearly linear model and unimodal, symmetric input distributions and a Gaussian output, which is the case in the analyzed PSHA. In contrast to that, the suggested upper bounding of global sensitivities is a more robust method without having these strong restrictions.

An example was given to illustrate the benefits that the derivative-based GSA methods have in the context of PSHA. Assuming uncertain inputs, the computed hazard results are mainly influenced by the uncertainty in the stress parameter $\Delta\sigma$ for all cases, and to a significant extent by the uncertainty in κ_0 for large oscillator frequencies. This is due to the large uncertainties related to these inputs. Seismicity parameter β (decay rate), α (activity level), and geometrical spreading η have a substantial influence on the hazard results for low oscillator frequencies. The presented approach is flexible and can be easily adjusted for different settings. Its computational gain increases even with larger complexity of the PSHA. An implementation of the proposed methods for complex PSHA studies yields not only the classical hazard results but additionally the highly informative sensitivity estimates alongside. This is of great value for many applications within the field of seismic-hazard analysis and earthquake engineering.

Data and Resources

A comprehensive overview of algorithmic differentiation (AD) tools, AD applications, and the underlying AD methodology is provided at http://www.autodiff.org (last accessed May 2016). AD of the computer source code of this study has been done by using AD tool Tapenade http://www-sop.inria.fr/tropics/ (last accessed May 2016). The FORTRAN source code of the Stochastic-Method SIMulation provided by David Boore (http://www.daveboore.com/software_online.html, last accessed May 2016) has been modified and used for ground-motion simulation.

Acknowledgments

This research has been partly done with financial support by Helmholtz Graduate Research School GeoSim, Christian Molkenthin is very thankful for the provided scholarship. The authors express their great appreciation to Nikos Giannotis, Carsten Riggelsen, Conny Hammer, Sanjay Singh Bora, and Galina Kulikova for very helpful discussions and for their valuable and constructive suggestions, which led to significant improvements of the article. We are grateful to Marco Pagani and an anonymous reviewer as well as to Associate Editor John Douglas for their valuable suggestions and comments, which helped to improve the article. This work was partly conducted in the Research Training Group GRK1364 "Shaping Earth's Surface in a variable Environment" funded by the German Research Foundation, cofinanced by the federal state of Brandenburg and the University of Potsdam.

References

Atkinson, G. M., and D. M. Boore (2006). Earthquake ground-motion prediction equations for eastern North America, *Bull. Seismol. Soc. Am.* **96,** 2181–2205.

Baydin, A. G., B. A. Pearlmutter, A. A. Radul, and J. M. Siskind (2015). Automatic differentiation in machine learning: A survey, 28, http://arxiv.org/abs/1502.05767 (last accessed May 2016).

Bommer, J. J. (2012). Challenges of building logic trees for probabilistic seismic hazard analysis, *Earthq. Spectra* **28,** 1723–1735.

Bommer, J. J., and F. Scherbaum (2008). The use and misuse of logic trees in probabilistic seismic hazard analysis, *Earthq. Spectra* **24,** 997–1009.

Boore, D. M. (2003). Simulation of ground motion using the stochastic method, *Pure Appl. Geophys.* **160,** 635–676.

Boore, D. M., and W. B. Joyner (1997). Site amplifications for generic rock sites, *Bull. Seismol. Soc. Am.* **87,** 327–341.

Bora, S. S., F. Scherbaum, N. Kuehn, and P. Stafford (2016). On the relationship between Fourier and response spectra: Implications for the adjustment of empirical ground-motion prediction equations (GMPEs), *Bull. Seismol. Soc. Am.* **106,** 1235–1253.

Bora, S. S., F. Scherbaum, N. Kuehn, P. Stafford, and B. Edwards (2015). Development of a response spectral ground-motion prediction equation (GMPE) for seismic-hazard analysis from empirical Fourier spectral and duration models, *Bull. Seismol. Soc. Am.* **105,** 2192–2218.

Borgonovo, E. (2006). Measuring uncertainty importance: Investigation and comparison of alternative approaches, *Risk Anal.* **26,** 1349–1361.

Borgonovo, E., and E. Plischke (2016). Sensitivity analysis: A review of recent advances, *Eur. J. Oper. Res.* **248,** 869–887.

Bratley, P., B. L. Fox, and H. Niederreiter (1992). Implementation and tests of low-discrepancy sequences, *ACM Trans. Model. Comput. Simulat.* **2,** no. 3, 195–213.

Brune, J. N. (1970). Tectonic stress and the spectra of seismic shear waves from earthquakes, *J. Geophys. Res.* **75,** 4997–5009.

Brune, J. N. (1971). Correction to "Tectonic stress and the spectra, of seismic shear waves from earthquakes", *J. Geophys. Res.* **76,** 5002–5002.

Budnitz, R. J., G. Apostolakis, D. M. Boore, L. S. Cluff, K. J. Coppersmith, C. A. Cornell, and P. A. Morris (1997). Recommendations for probabilistic seismic hazard analysis: Guidance on uncertainty and use of experts, *U.S. Nuclear Regulatory Commission Rept. NUREG/CR-6372*.

Cacuci, D. G., and M. Ionescu-Bujor (2004). A comparative review of sensitivity and uncertainty analysis of large-scale systems—II: Statistical methods, *Nucl. Sci. Eng.* **147,** 204–217.

Castaings, W., D. Dartus, F. X. Le Dimet, and G. M. Saulnier (2009). Sensitivity analysis and parameter estimation for distributed hydrological modeling: Potential of variational methods, *Hydrol. Earth Syst. Sci.* **13,** 503–517.

Cornell, C. A. (1968). Engineering seismic risk analysis, *Bull. Seismol. Soc. Am.* **58,** 1583–1606.

Cotton, F., R. Archuleta, and M. Causse (2013). What is sigma of the stress drop? *Seismol. Res. Lett.* **84,** 42–48.

Cotton, F., F. Scherbaum, J. J. Bommer, and H. Bungum (2006). Criteria for selecting and adjusting ground-motion models for specific target regions: Application to central Europe and rock sites, *J. Seismol.* **10,** 137–156.

De Rocquigny, E., N. Devictor, and S. Tarantola (Editors) (2008). *Uncertainty in Industrial Practice: A Guide to Quantitative Uncertainty Management*, John Wiley & Sons, Chichester, United Kingdom.

Douglas, J., S. Akkar, G. Ameri, P. Y. Bard, D. Bindi, J. J. Bommer, S. S. Bora, F. Cotton, B. Derras, M. Hermkes, *et al.* (2014). Comparisons among the five ground-motion models developed using RESORCE for the prediction of response spectral accelerations due to earthquakes in Europe and the Middle East, *Bull. Earthq. Eng.* **12,** 341–358.

Douglas, J., B. Edwards, V. Convertito, N. Sharma, A. Tramelli, D. Kraaijpoel, B. M. Cabrera, N. Maercklin, and C. Troise (2013). Predicting ground motion from induced earthquakes in geothermal areas, *Bull. Seismol. Soc. Am.* **103,** 1875–1897.

Douglas, J., T. Ulrich, D. Bertil, and J. Rey (2014). Comparison of the ranges of uncertainty captured in different seismic-hazard studies, *Seismol. Res. Lett.* **85,** 977–985.

Drouet, S., and F. Cotton (2015). Regional stochastic GMPEs in low-seismicity areas: Scaling and aleatory variability analysis—Application to the French Alps, *Bull. Seismol. Soc. Am.* **105,** 1883–1902.

Edwards, B., and D. Fah (2013). A stochastic ground-motion model for Switzerland, *Bull. Seismol. Soc. Am.* **103,** 78–98.

Fournier, D. A., H. J. Skaug, J. Ancheta, J. Ianelli, A. Magnusson, M. N. Maunder, A. Nielsen, and J. Sibert (2012). AD model builder: Using automatic differentiation for statistical inference of highly parameterized complex nonlinear models, *Optim. Meth. Software* **27,** 233–249.

Griewank, A. (2013). On stable piecewise linearization and generalized algorithmic differentiation, *Optim. Meth. Software* **28,** 1139–1178.

Griewank, A., and A. Walther (2008). *Evaluating Derivatives: Principles and Techniques of Algorithmic Differentiation*, Second Ed., Society for Industrial and Applied Mathematics, Philadelphia, Pennsylvania, 438 pp.

Hascoet, L., and V. Pascual (2013). The tapenade automatic differentiation tool: Principles, model, and specification, *ACM Trans. Math. Software* **39,** 20.

Homma, T., and A. Saltelli (1996). Importance measures in global sensitivity analysis of nonlinear models, *Reliab. Eng. Syst. Saf.* **52,** 1–17.

Ionescu-Bujor, M., and D. G. Cacuci (2004). A comparative review of sensitivity and uncertainty analysis of large-scale systems—I: Deterministic methods, *Nucl. Sci. Eng.* **147,** 189–203.

Iooss, B., and P. Lemaître (2015). A review on global sensitivity analysis methods, in *Uncertainty Management in Simulation-Optimization of Complex Systems*, Springer, New York, New York, 101–122.

Kramer, S. L. (1996). *Geotechnical Earthquake Engineering*, Prentice Hall Civil Engineering and Engineering Mechanics Series, Englewood Cliffs, New Jersey, 653 pp.

Kucherenko, S., and B. Iooss (2016). Derivative-based global sensitivity measures, in *Handbook of Uncertainty Quantification*, Springer International Publishing, Cham, Switzerland, pp. 1–24.

Kucherenko, S., D. Albrecht, and A. Saltelli (2015). Exploring multi-dimensional spaces: A comparison of Latin hypercube and quasi Monte Carlo sampling techniques, *The 8th IMACS Seminar on Monte Carlo Methods*, 1–32.

Kucherenko, S., B. Feil, N. Shah, and W. Mauntz (2011). The identification of model effective dimensions using global sensitivity analysis, *Reliab. Eng. Syst. Saf.* **96,** 440–449.

Kulkarni, R. B., R. R. Youngs, and K. J. Coppersmith (1984). Assessment of confidence intervals for results of seismic hazard analysis, *Proc. of Eighth World Conference on Earthquake Engineering*, San Francisco, California, 21–28 July, Vol. 1, 263–270.

Lamboni, M., B. Iooss, A. L. Popelin, and F. Gamboa (2013). Derivative-based global sensitivity measures: General links with Sobol' indices and numerical tests, *Math. Comput. Simulat.* **87,** 45–54.

Massmann, C., and H. Holzmann (2012). Analysis of the behavior of a rainfall-runoff model using three global sensitivity analysis methods evaluated at different temporal scales, *J. Hydrol.* **475,** 97–110.

McGuire, R. K. (2004). *Seismic Hazard and Risk Analysis*, Earthquake Engineering Research Institute, Oakland, California.

McKay, M. D. (1995). Evaluating prediction uncertainty, *U.S. Nuclear Regulatory Commission Rept. NUREG/CR-6311*, Los Alamos National Laboratory.

Molkenthin, C., F. Scherbaum, A. Griewank, N. M. Kuehn, and P. J. Stafford (2014). A study of the sensitivity of response spectral amplitudes on seismological parameters using algorithmic differentiation, *Bull. Seismol. Soc. Am.* **104,** 2240–2252.

Molkenthin, C., F. Scherbaum, A. Griewank, N. M. Kuehn, P. J. Stafford, and H. Leovey (2015). Sensitivity of probabilistic seismic hazard obtained by algorithmic differentiation: A feasibility study, *Bull. Seismol. Soc. Am.* **105,** 1810–1822.

Niederreiter, H. (1992). Random number generation and quasi-Monte Carlo methods, in *CBMS-NSF Regional Conference Series in Applied Mathematics*, Vol. 63, Society for Industrial and Applied Mathematics (SIAM), Philadelphia, Pennsylvania.

Oakley, J. E., and A. O'Hagan (2004). Probabilistic sensitivity analysis of complex models: A Bayesian approach, *J. Roy. Stat. Soc. B. Stat. Meth.* **66,** 751–769.

Ordaz, M. (2004). Some useful integrals in seismic hazard analysis, *Bull. Seismol. Soc. Am.* **93,** 1012–1033.

Pappenberger, F., K. J. Beven, M. Ratto, and P. Matgen (2008). Multi-method global sensitivity analysis of flood inundation models, *Adv. Water Resour.* **31,** 1–14.

Paskov, S. H., and J. F. Traub (1995). Faster valuation of financial derivatives, *J. Portfolio Manag.* **22,** no. 1, 113–123.

Plischke, E., E. Borgonovo, and C. L. Smith (2013). Global sensitivity measures from given data, *Eur. J. Oper. Res.* **226,** 536–550.

Rakovec, O., M. C. Hill, M. P. Clark, A. H. Weerts, A. J. Teuling, and R. Uijlenhoet (2014). Distributed Evaluation of Local Sensitivity Analysis (DELSA), with application to hydrologic models, *Water Resour. Res.* **50,** 409–426.

Razavi, S., and H. V. Gupta (2015). What do we mean by sensitivity analysis? The need for comprehensive characterization of "global" sensitivity in Earth and environmental systems models, *Water Resour. Res.* **51,** 3070–3092.

Rietbrock, A., F. Strasser, B. Edwards, and B. Edwards (2013). A stochastic earthquake ground-motion prediction model for the United Kingdom, *Bull. Seismol. Soc. Am.* **103,** 57–77.

Roustant, O., J. Fruth, B. Iooss, and S. Kuhnt (2014). Crossed-derivative based sensitivity measures for interaction screening, *Math. Comput. Simulat.* **105,** 105–118.

Saltelli, A. (2002). Making best use of model evaluations to compute sensitivity indices, *Comput. Phys. Comm.* **145,** 280–297.

Saltelli, A., P. Annoni, I. Azzini, F. Campolongo, M. Ratto, and S. Tarantola (2010). Variance based sensitivity analysis of model output. Design and estimator for the total sensitivity index, *Comput. Phys. Comm.* **181,** 259–270.

Saltelli, A., K. Chan, and E. M. Scott (Editors) (2000). *Sensitivity Analysis*, Wiley, New York, New York.

Saltelli, A., M. Ratto, T. Andres, F. Campolongo, J. Cariboni, D. Gatelli, M. Saisana, and S. Tarantola (2008). *Global Sensitivity Analysis: The Primer*, John Wiley & Sons Ltd, Chichester, England, 312 pp., ISBN: 978-0-470-05997-5.

Sambridge, M., P. Rickwood, N. Rawlinson, and S. Sommacal (2007). Automatic differentiation in geophysical inverse problems, *Geophys. J. Int.* **170,** 1–8.

Scherbaum, F., J. J. Bommer, H. Bungum, F. Cotton, and N. Abrahamson (2005). Composite ground-motion models and logic trees: Methodology, sensitivities, and uncertainties, *Bull. Seismol. Soc. Am.* **95,** 1575–1593.

Skaug, H. J., and J. Yu (2014). A flexible and automated likelihood based framework for inference in stochastic volatility models, *Comput. Stat. Data Anal.* **76,** 642–654.

Sobol', I. M. (1990). Estimation of the sensitivity of nonlinear mathematical models, *Mat. Model.* **2,** no. 1, 112–118 (in Russian).

Sobol', I. M. (1998). On quasi-Monte Carlo integrations, *Math. Comput. Simulat.* **47,** no. 2, 103–112.

Sobol', I. M. (2001). Global sensitivity indices for nonlinear mathematical models and their Monte Carlo estimates, *Math. Comput. Simulat.* **55,** 271–280.

Sobol', I. M., and S. Kucherenko (2009). Derivative based global sensitivity measures and their link with global sensitivity indices, *Math. Comput. Simulat.* **79,** 3009–3017.

Sobol', I. M., D. Asotsky, A. Kreinin, and S. Kucherenko (2011). Construction and comparison of high-dimensional Sobol' generators, *Wilmott* **2011,** 64–79.

Sobol', I. M., S. Tarantola, D. Gatelli, S. Kucherenko, and W. Mauntz (2007). Estimating the approximation error when fixing unessential factors in global sensitivity analysis, *Reliab. Eng. Syst. Saf.* **92,** 957–960.

United States Nuclear Regulatory Commission (USNRC) (2012). *Practical Implementation Guidelines for SSHAC Level 3 and 4 Hazard Studies, NUREG 2117*, Division of Engineering, Office of Nuclear Research, U.S. Nuclear Regulatory Commission, Washington D.C.

Yenier, E., and G. M. Atkinson (2015). Regionally adjustable generic ground-motion prediction equation based on equivalent point-source simulations: Application to central and eastern North America, *Bull. Seismol. Soc. Am.* **105,** 1989–2009.

Institute of Earth and Environmental Science
University of Potsdam
Karl-Liebknecht Street 24-25
14476 Potsdam, Germany
molkenthin@geo.uni-potsdam.de
fs@geo.uni-potsdam.de
(C.M., F.S.)

School of Mathematical Sciences and Information Technology
Yachaytech, Hacienda San Jose, Urcuqui
100119, Imbabura, Ecuador
griewank@yachaytech.edu.ec
(A.G.)

Department of Mathematics
Humboldt-University Berlin
Unter den Linden 6
10099 Berlin, Germany
leovey@math.hu-berlin.de
(H.L.)

Faculty of Engineering, Department of Chemical Engineering
Imperial College London
South Kensington Campus
London SW7 2AZ, United Kingdom
s.kucherenko@imperial.ac.uk
(S.K.)

German Research Center for Geosciences (GFZ)
Helmholtzstraße 6/7
14467 Potsdam, Germany
fabrice.cotton@gfz-potsdam.de
(F.C.)

Manuscript received 9 June 2016;
Published Online 7 March 2017